

**Lithium achieves sequence selective ring-opening terpolymerisation (ROTERP)
of ternary monomer mixtures**

Susanne Rupf,^{a,#} Patrick Pröhm,^{a,#} Alex J. Plajer^{a,*}

^a Institut für Chemie und Biochemie, Freie Universität Berlin, Fabeckstraße 34-36,
14195 Berlin; # equal contribution; [*email: plajer@zedat.fu-berlin.de](mailto:plajer@zedat.fu-berlin.de)

Table of contents

Section S1: Methods.....	3
Section S2: ROTERP procedure and details	4
Section S3: Polymer characterisation data	5
Section S4: SEC traces.....	18
Section S5: Synthesis, characterisation and reactivity of model MTC	21
Section S6: Switchable Catalysis.....	32
Section S7: Degradation Experiments	40
Section S8: Crystallography	43
Section S9: Bibliography	46

Section S1: Methods

Solvents and reagents were obtained from commercial sources and used as received unless stated otherwise. If “dried solvents” were used these were obtained by different procedures. Toluene, EtOH, n-hexane, n-pentane and CH₂Cl₂ were prepared by using an MBraun Solvent Purification System MB-SPS 800 filled with Al₂O₃. Et₂O was dried over Na/benzophenone and THF was dried over K/benzophenone under argon. The CDCl₃ was dried over CaH₂ and d₈-THF over sodium prior to vacuum transfer onto 4 Å sieves followed by three freeze pump thaw degassing cycles. ¹H, ¹³C{¹H}, and ⁷Li NMR spectra were recorded by using a Jeol JNM-ECA 400II, Bruker Advance 600 and 700 MHz spectrometer. ¹H and ¹³C{¹H} chemical shifts are referenced to the residual proton resonance of the deuterated solvents and ⁷Li{¹H} chemical shifts are referenced to an internal reference capillary containing LiO₃SCF₃ in d₆-acetone (alongside a PPh₃ ³¹P reference and PhF ¹⁹F reference).

Epoxides, CS₂ and ε-DL were dried over calcium hydride at room temperature for 3 days, vacuum transferred (for CHO and ε-DL fractionally distilled under static vacuum) followed by three freeze pump thaw degassing cycles and stored inside an argon filled glovebox prior to use. Phtalic thioanhydride was synthesized according to the literature procedure and (for runs Table 1 #5 and #6) this was then purified by recrystallisation from ^tBuOMe followed by recrystallisation from CHCl₃ and two sublimation under dynamic vacuum at 90°C and was stored inside an argon filled glovebox prior to use.^[1]

UV-visible spectra were collected on a Varian Cary 50 UV spectrometer.

Infrared spectra were measured using a Thermo-Nicolet Nexus 670 FTIR spectrometer with DuraSampl IR accessory in total reflection at room temperature.

The molecular mass and polydispersity of the polymers were determined by a Waters 1515 size exclusion chromatography (SEC) instrument equipped with two linear PLgel columns (Mixed-C) following a guard column and a differential refractive index detector using tetrahydrofuran as the eluent at a flow rate of 1.0 mL/min at 30 °C and a series of narrow polystyrene standards for the calibration of the columns. Each polymer sample was dissolved in HPLC-grade THF (6 mg/mL) and filtered through a 0.20 μm porous filter frit prior to analysis.

Polymer films for refractive index determination were spun from a Vacuum Spin Coater (SCE 150). 100 μL of terpolymers in CH₂Cl₂ (20 mg/mL) was dropped onto a silicon slice and the speed of the spin coater was then raised to 3000 r/min lasting for 1 min, affording a film of approximately 100 – 200 nm. Spectroscopic ellipsometry (SE) was performed on a SENpro ellipsometer (wavelength 350 – 1050 nm) and evaluated with SpectraRay 3 (Version 5.3.2.1853) software from SENTECH instruments GmbH (Berlin, Germany).

High-resolution ESI mass spectra were obtained using a Waters UPLC-Synapt G2-S HDMS.

Section S2: ROTERP procedure and details

Terpolymerization protocol: In an argon-filled glovebox, LiHMDS (an optionally BnOH) was dissolved in butylene oxide and the mixture was transferred to a flame dried vial equipped with a flame dried stirrer bar and sealed with a melamine cap containing a Teflon inlay. CS₂ and PTA were then added and the vial was brought outside the glovebox and placed in a pre-heated oil bath at 80°C for the specified time. In cases where the reaction progress was monitored, the vial was rapidly cooled to room temperature with a dry ice cooling bath and brought inside an argon-filled glovebox before the aliquot was removed. At the specified end point of the reaction, the polymer was isolated by adding the polymerisation mixture to 200 mL of acidified MeOH (20 µL concentrated HCl per 200 mL MeOH) resulting in the precipitation of the yellow product. After two further precipitations from DCM/MeOH, the polymer was isolated by filtration and dried in a vacuum oven set to 60 °C.

Section S3: Polymer characterisation data

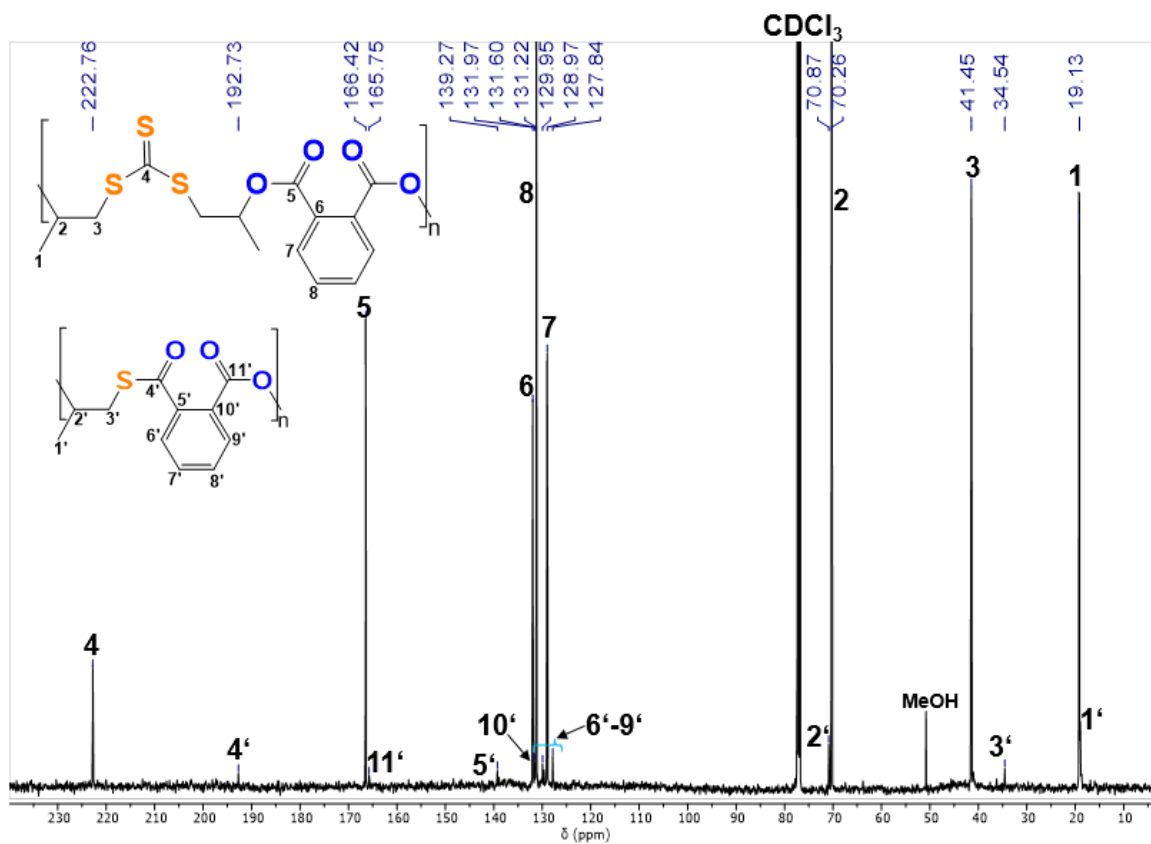


Figure S 1: $^{13}\text{C}\{^1\text{H}\}$ NMR spectrum (126 MHz, CDCl₃, 25°C) of terpolymer corresponding to table 1, run #3.

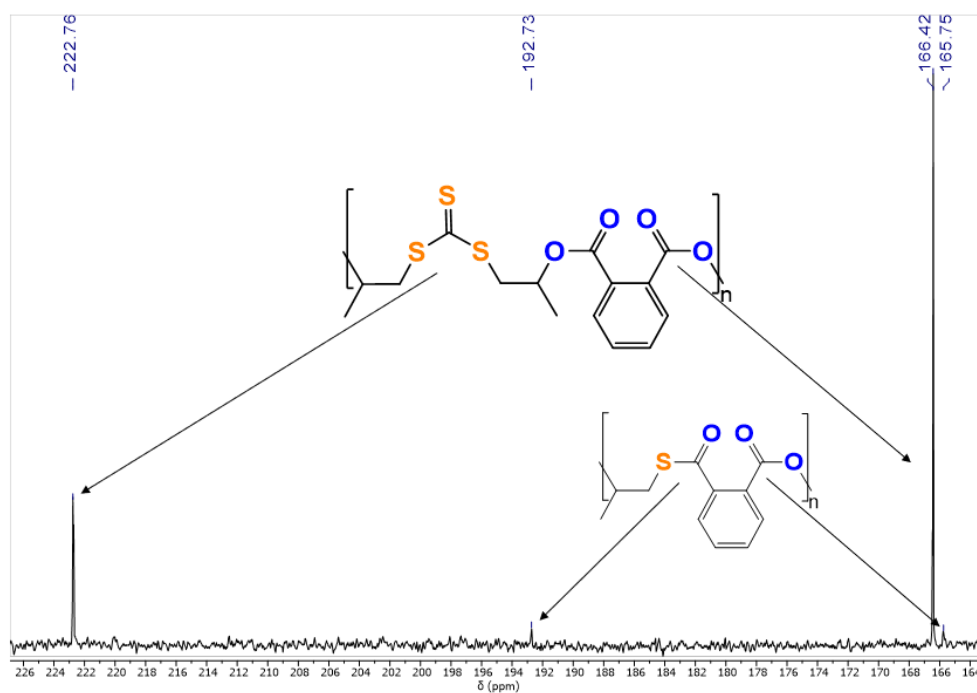


Figure S 2: Zoom into carbonyl region of the $^{13}\text{C}\{^1\text{H}\}$ NMR spectrum (126 MHz, CDCl₃, 25°C) of terpolymer corresponding to table 1, run #3.

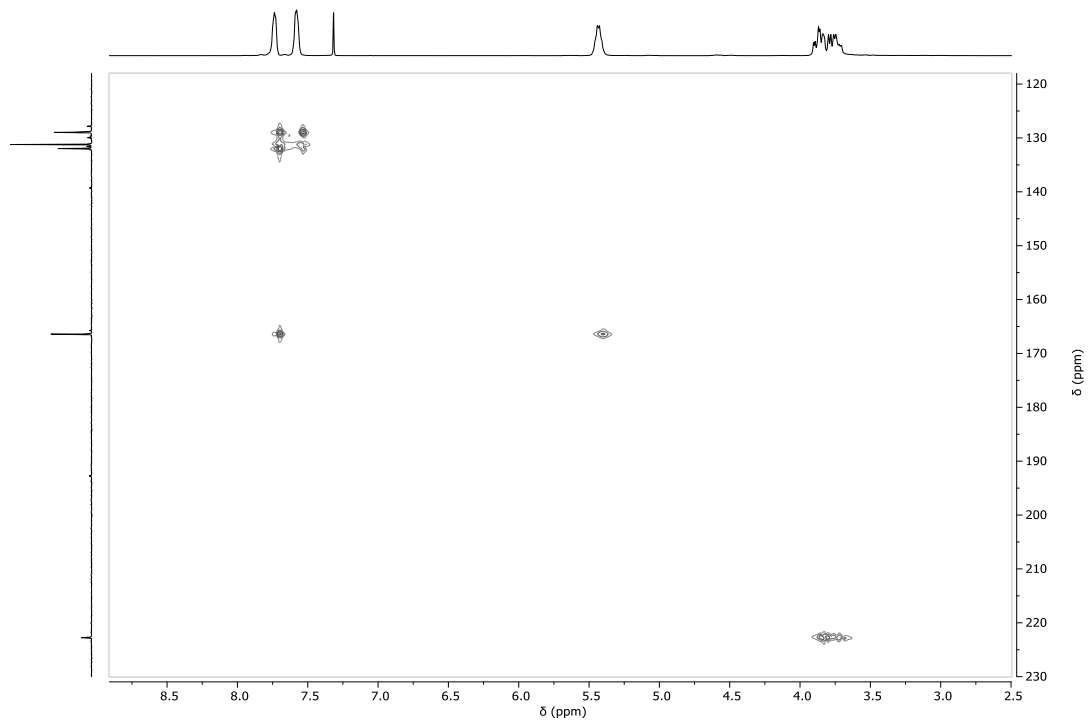


Figure S 3: $^1\text{H} - ^{13}\text{C}$ HMBC NMR spectrum (CDCl_3 , 25°C) of terpolymer corresponding to table 1, run #3.

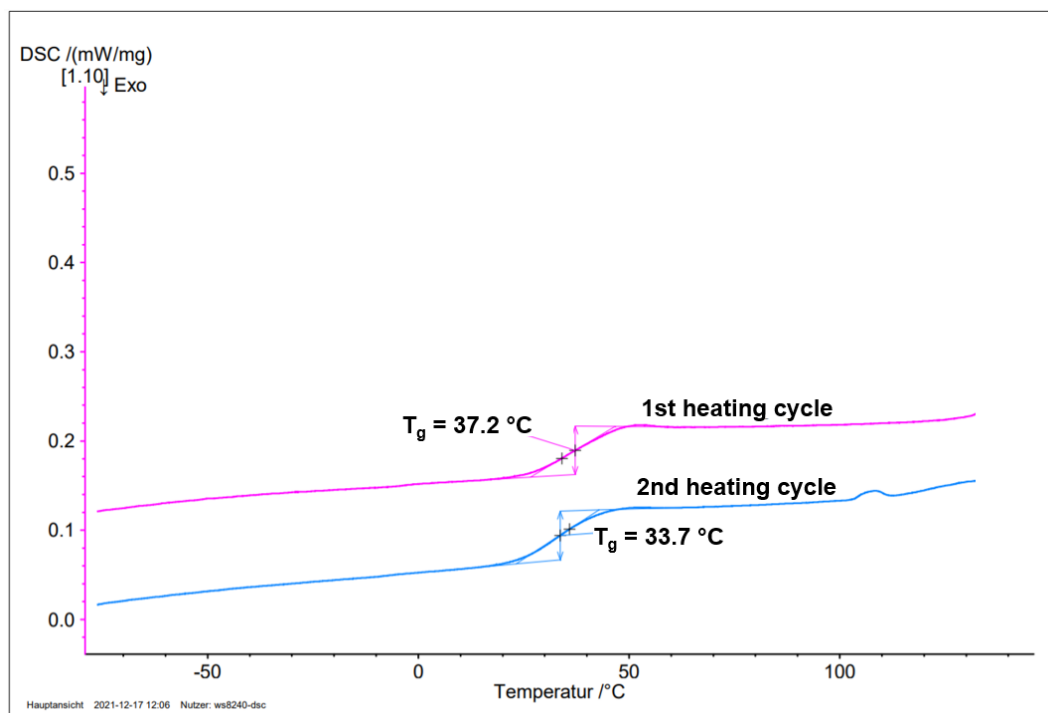


Figure S 4: DSC heating curve of terpolymer corresponding to table 1, run #4.

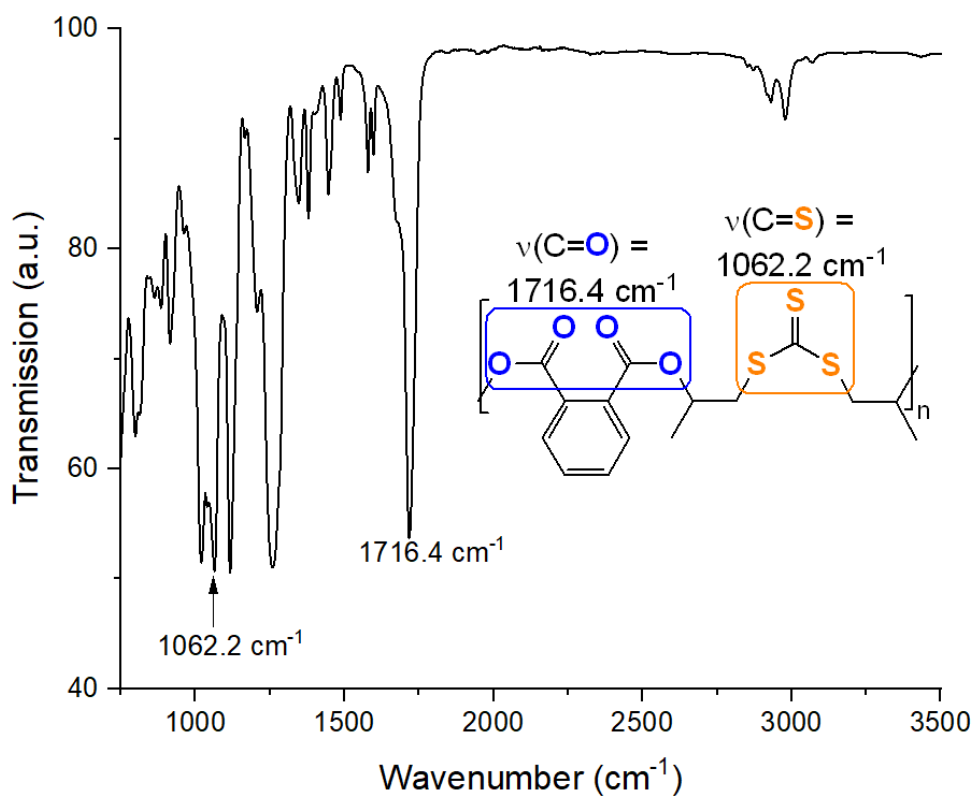


Figure S 5: FT ATRIR Spectrum of PTA/BO/CS₂ terpolymer corresponding to table 1, run #4.

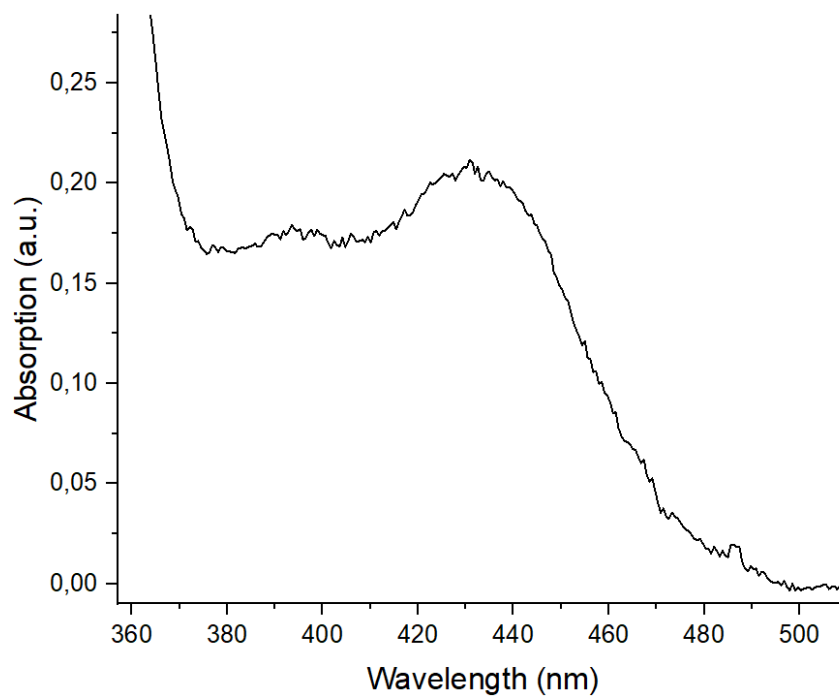


Figure S 6a: Zoom into the UVVIS spectrum (DCM, 25°C) of terpolymer corresponding to table 1, run #4.

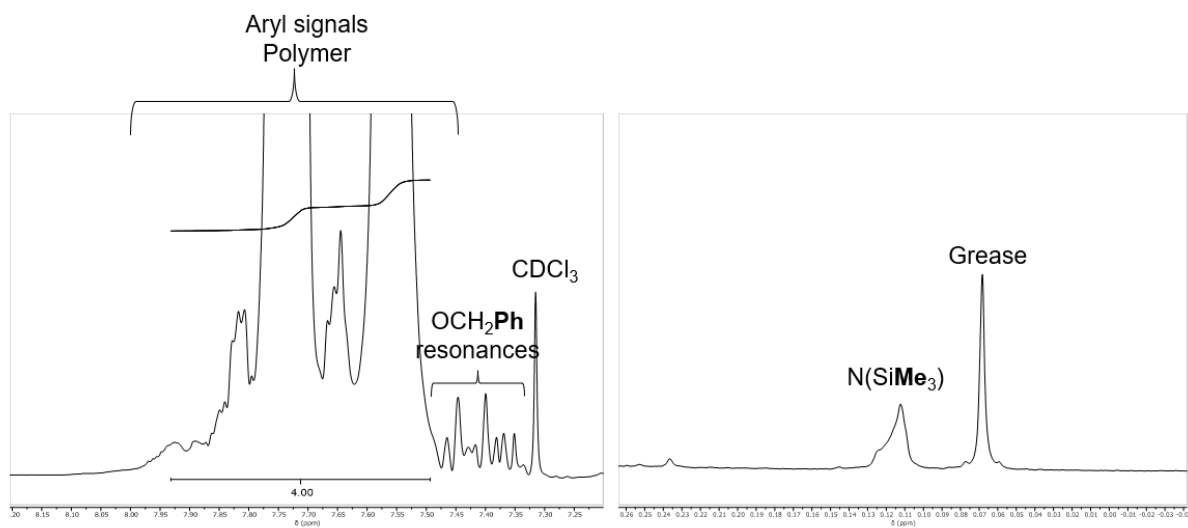


Figure S 6b: Zoom into the end-group resonances of of (left) a ROTERP reaction initiated from LiOBn and (right) initiated from LiHMDS.

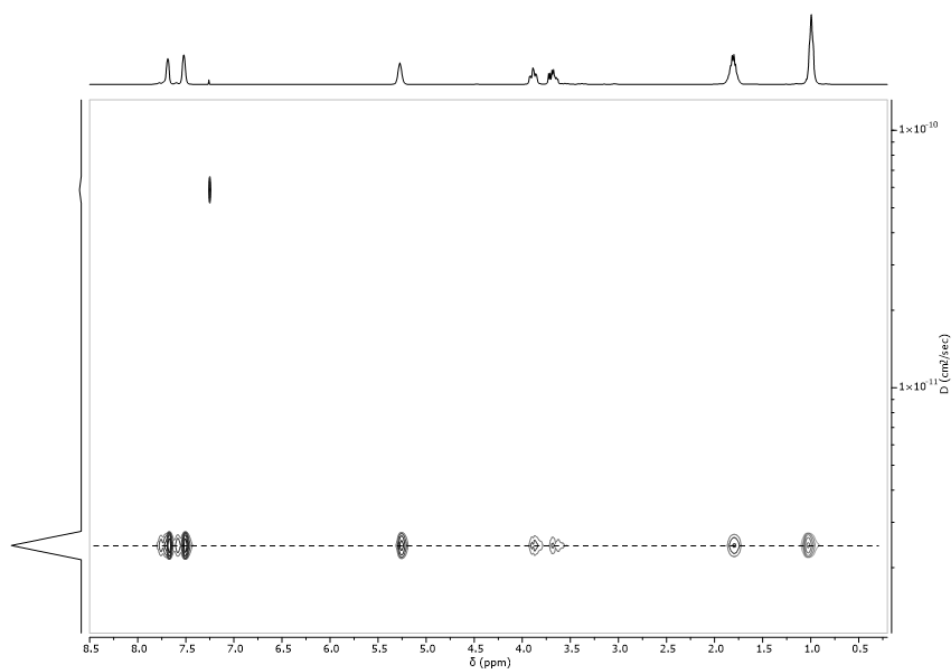


Figure S 6c: DOSY NMR spectrum (126 MHz, CDCl₃, 25°C) of terpolymer corresponding to table 1, run #3

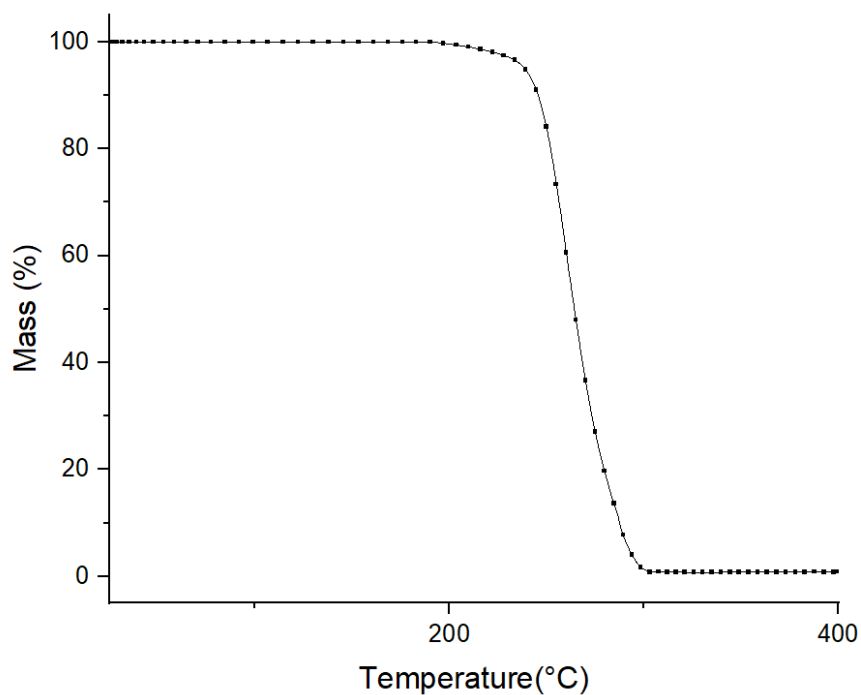


Figure S 7: TGA of terpolymer corresponding to table 1, run #4.

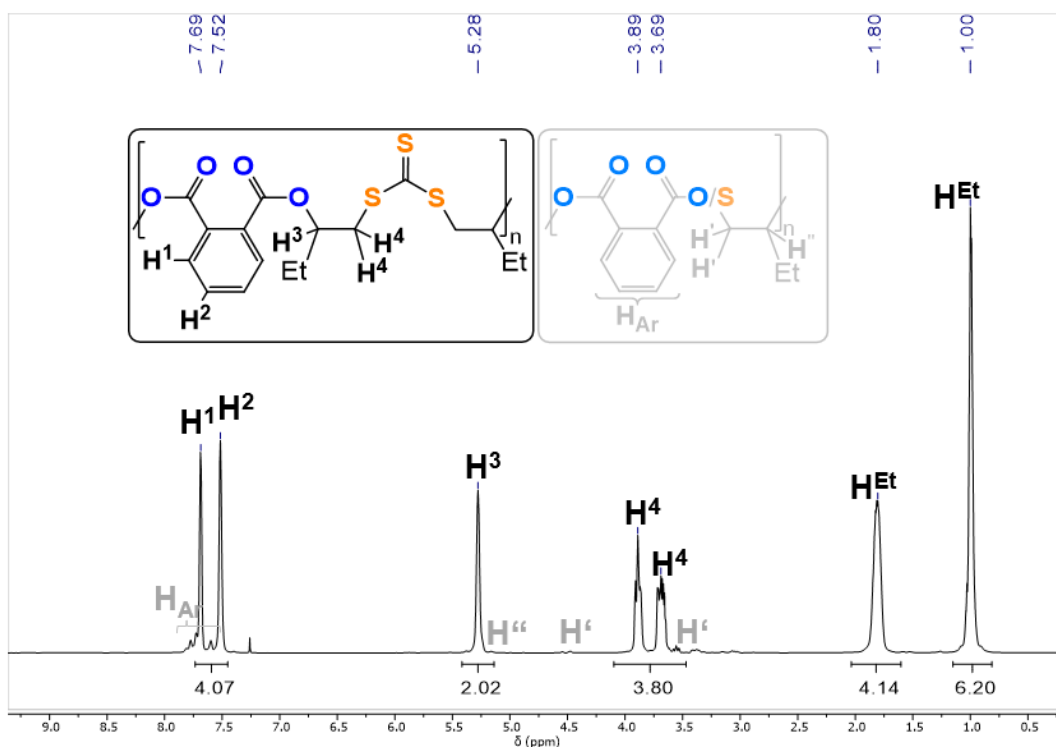


Figure S 8: ¹H NMR spectrum (400 MHz, CDCl₃, 25°C) of terpolymer corresponding to table 1, run #9.

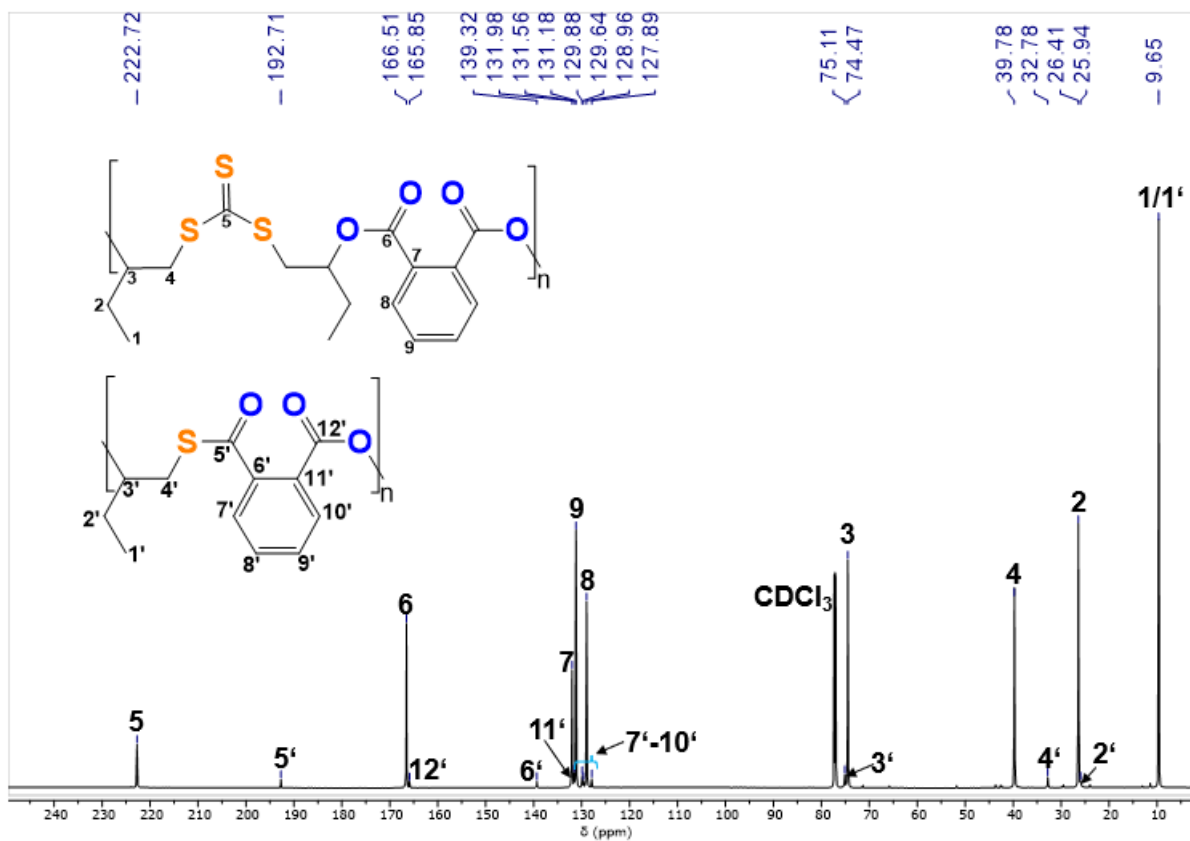


Figure S 9: $^{13}\text{C}\{^1\text{H}\}$ NMR spectrum (126 MHz, CDCl_3 , 25°C) of terpolymer corresponding to table 1, run #9.

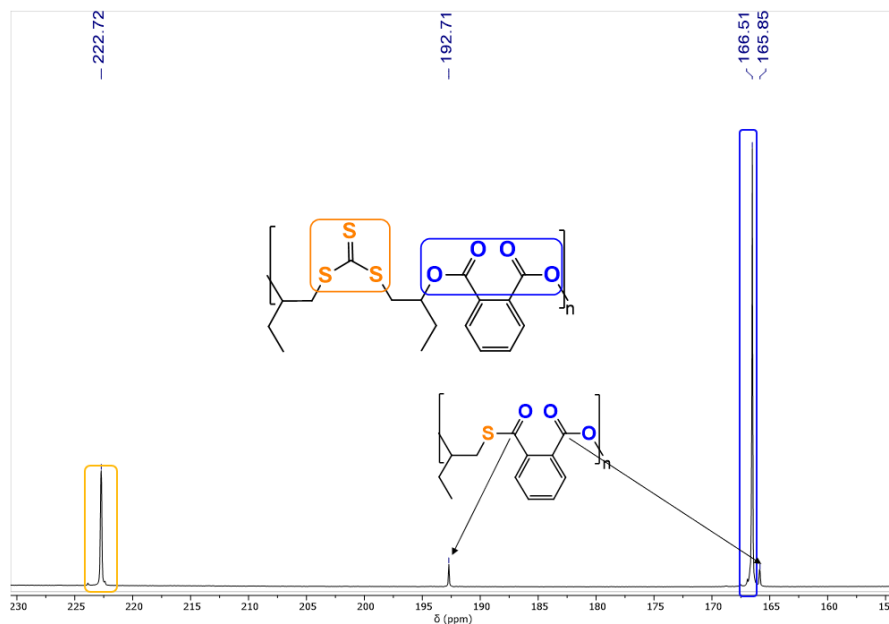


Figure S 10: Zoom into carbonyl region of the $^{13}\text{C}\{^1\text{H}\}$ NMR spectrum (126 MHz, CDCl_3 , 25°C) of terpolymer corresponding to table 1, run #9.

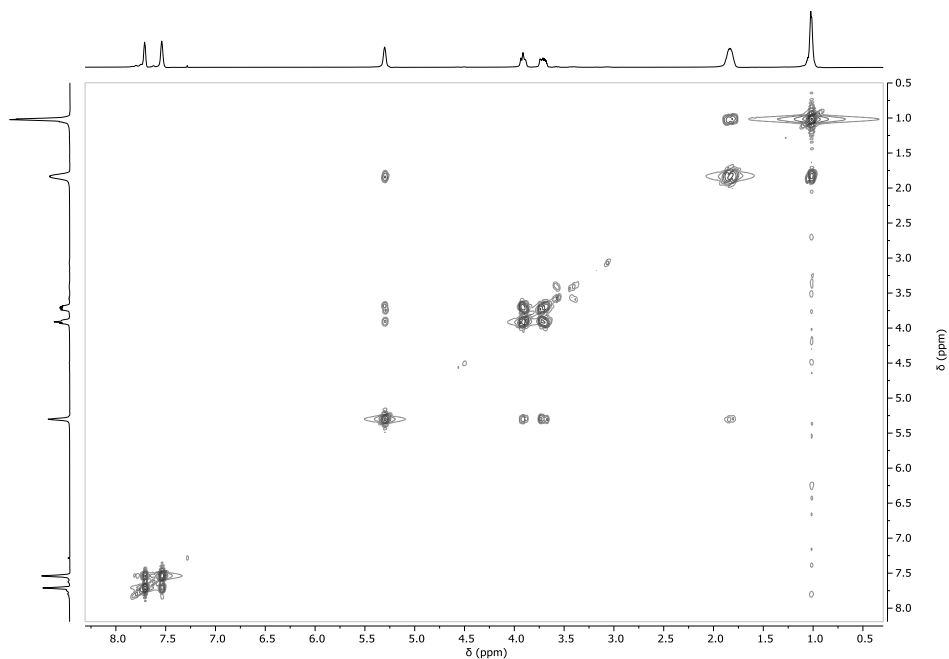


Figure S 11: $^1\text{H} - ^1\text{H}$ COSY NMR spectrum (CDCl_3 , 25°C) of terpolymer corresponding to table 1, run #9.

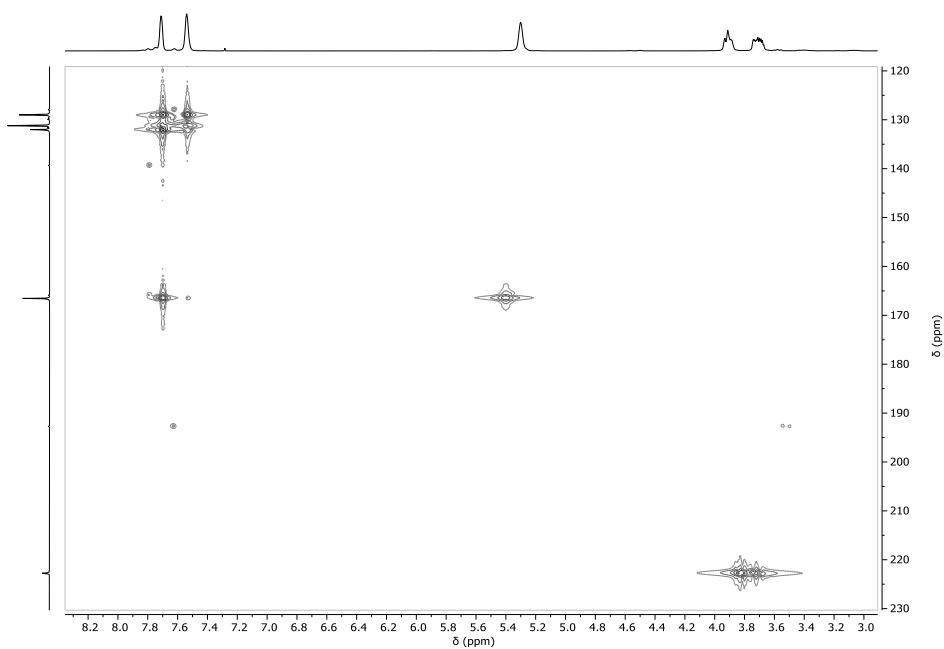


Figure S 12: $^1\text{H} - ^{13}\text{C}$ HMBC NMR spectrum (CDCl_3 , 25°C) of terpolymer corresponding to table 1, run #9.

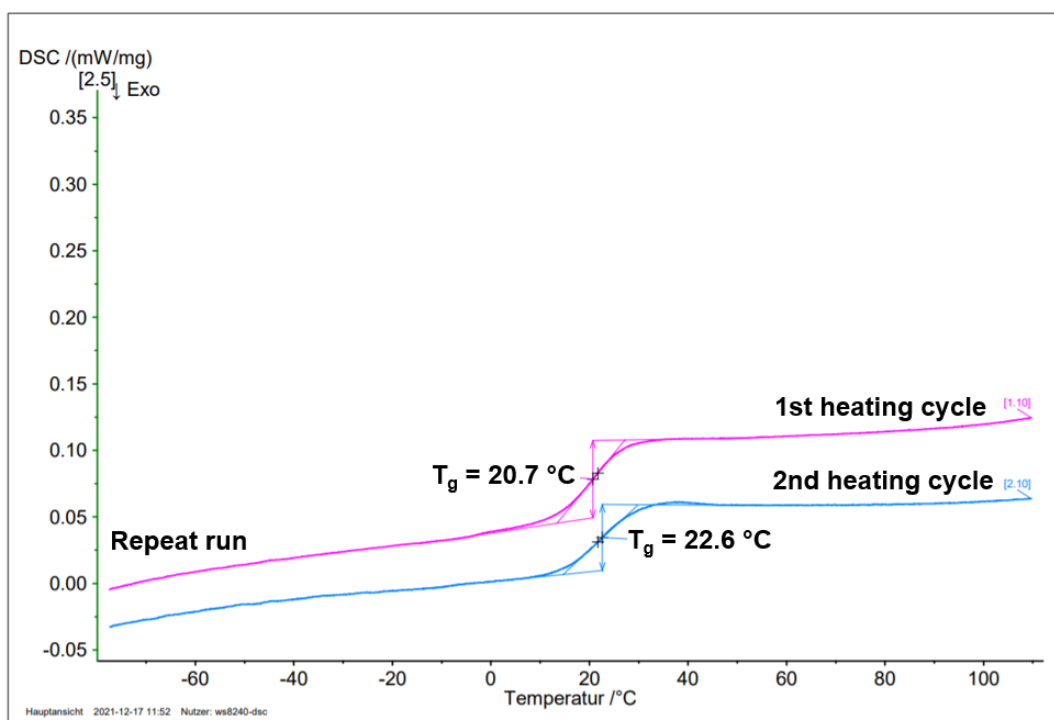


Figure S 13: DSC heating curve of terpolymer corresponding to table 1, run #9.

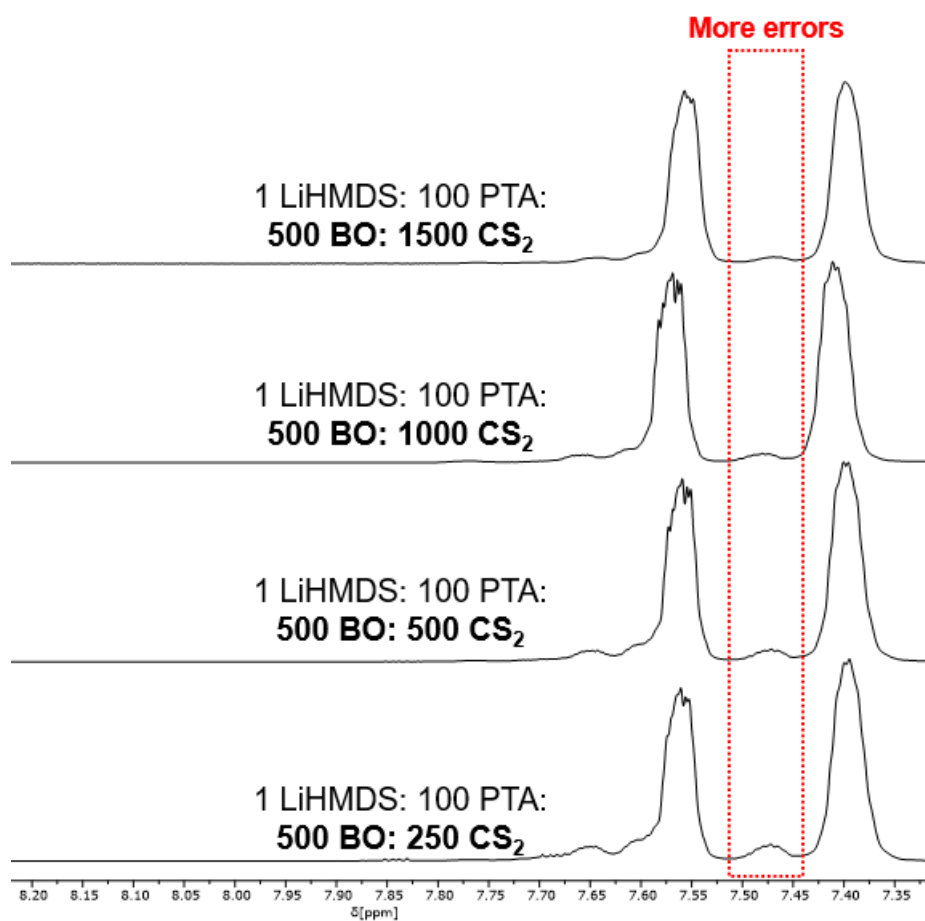


Figure S 14: Comparison of the aromatic region of the ^1H NMR spectra (400 MHz, CDCl_3 , 25°C) of terpolymers corresponding to table 1, run #7 to #10.

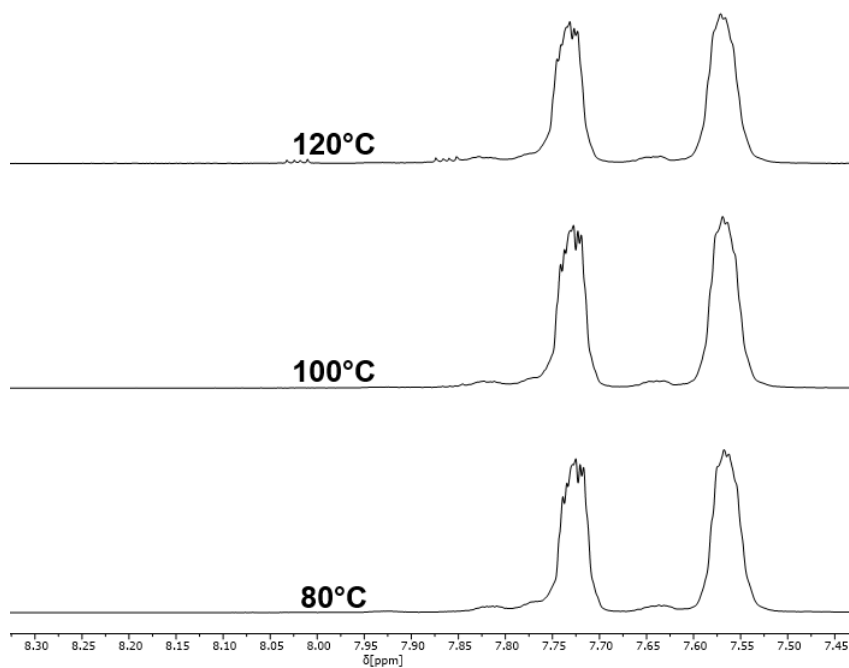


Figure S 15: Comparison of the aromatic region of the ^1H NMR spectra (400 MHz, CDCl_3 , 25°C) of crude terpolymers obtained at different reaction temperatures (loading as per Table 1 run #9).

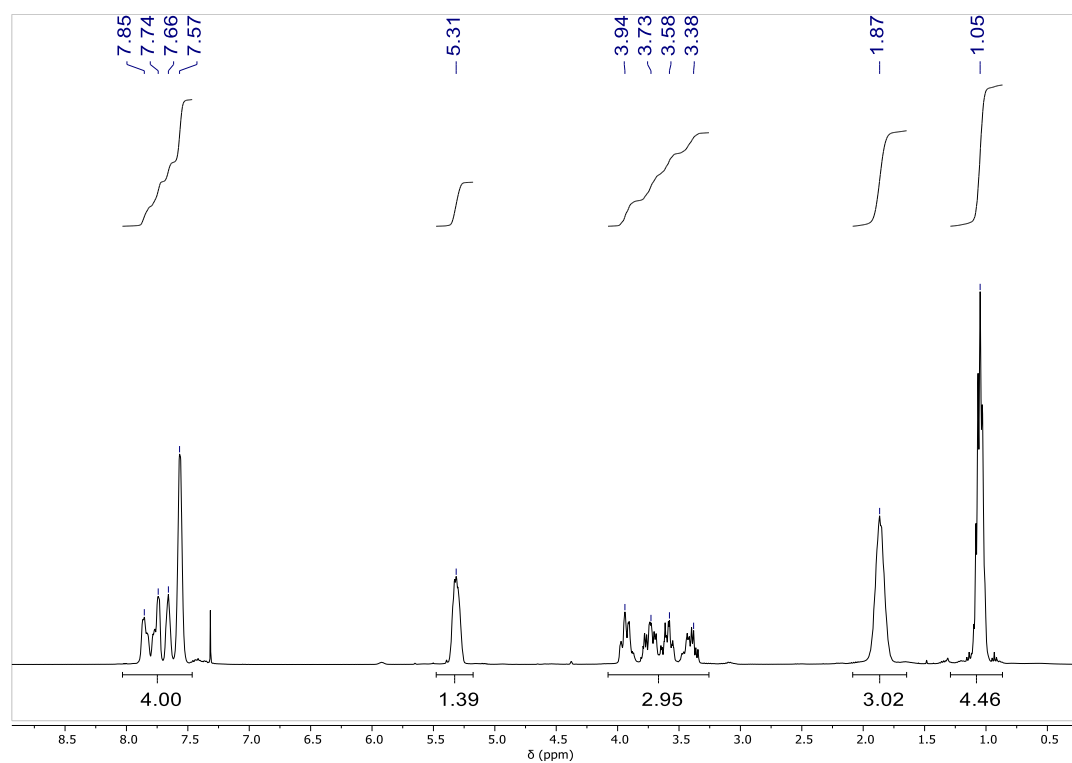


Figure S 16: ^1H NMR spectra (400 MHz, CDCl_3 , 25°C) of terpolymers corresponding to Table 1 run #12.

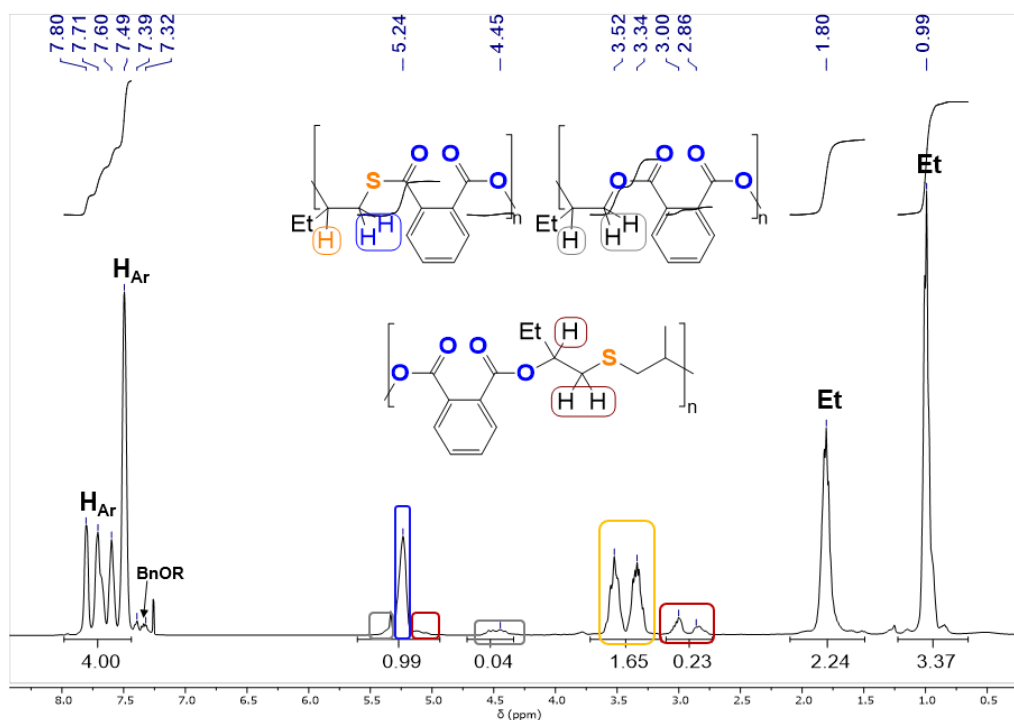


Figure S 17: ^1H NMR spectrum (400 MHz, CDCl_3 , 25°C) of copolymer corresponding to table 1, run #15.

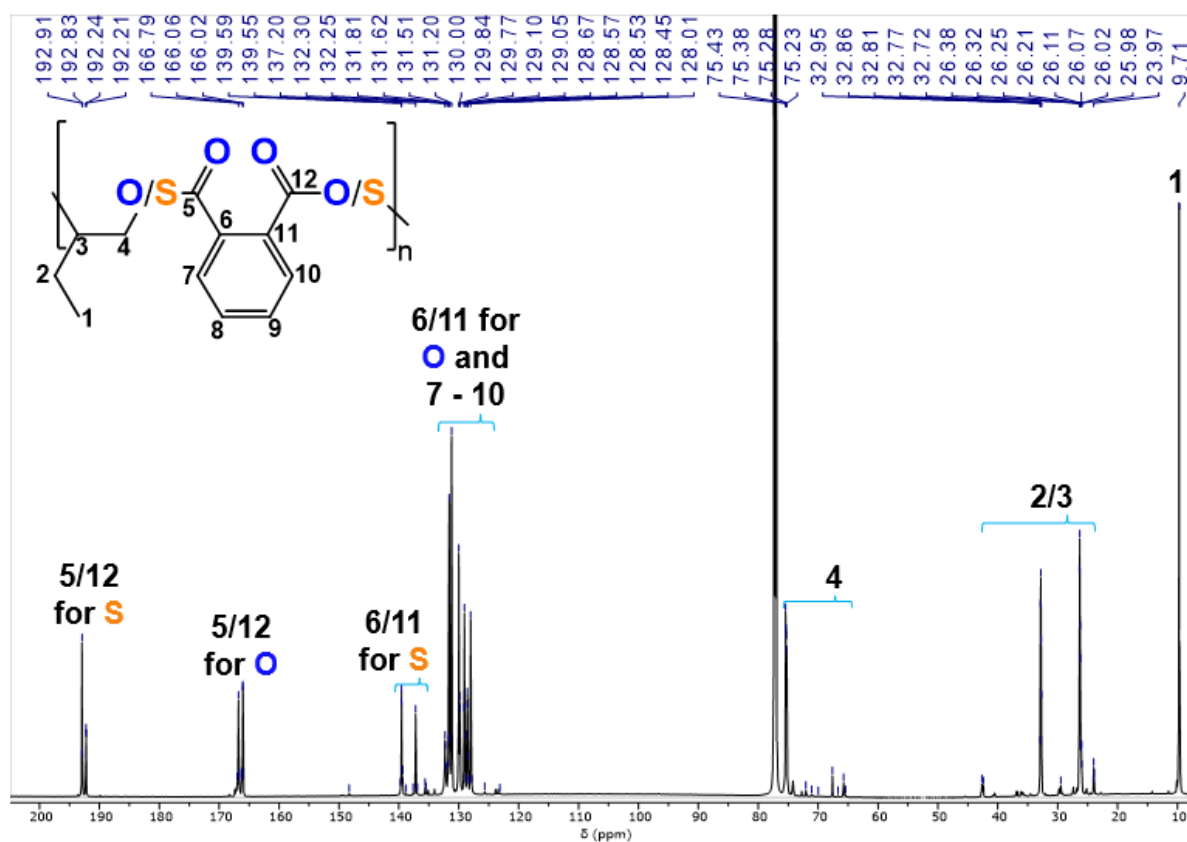


Figure S 18: $^{13}\text{C}\{^1\text{H}\}$ NMR spectrum (126 MHz, CDCl_3 , 25°C) of copolymer corresponding to table 1, run #15. Due to significant transesterification and O/S

exchange process as well as the presence of ether linkages unambiguous assignment was not possible.

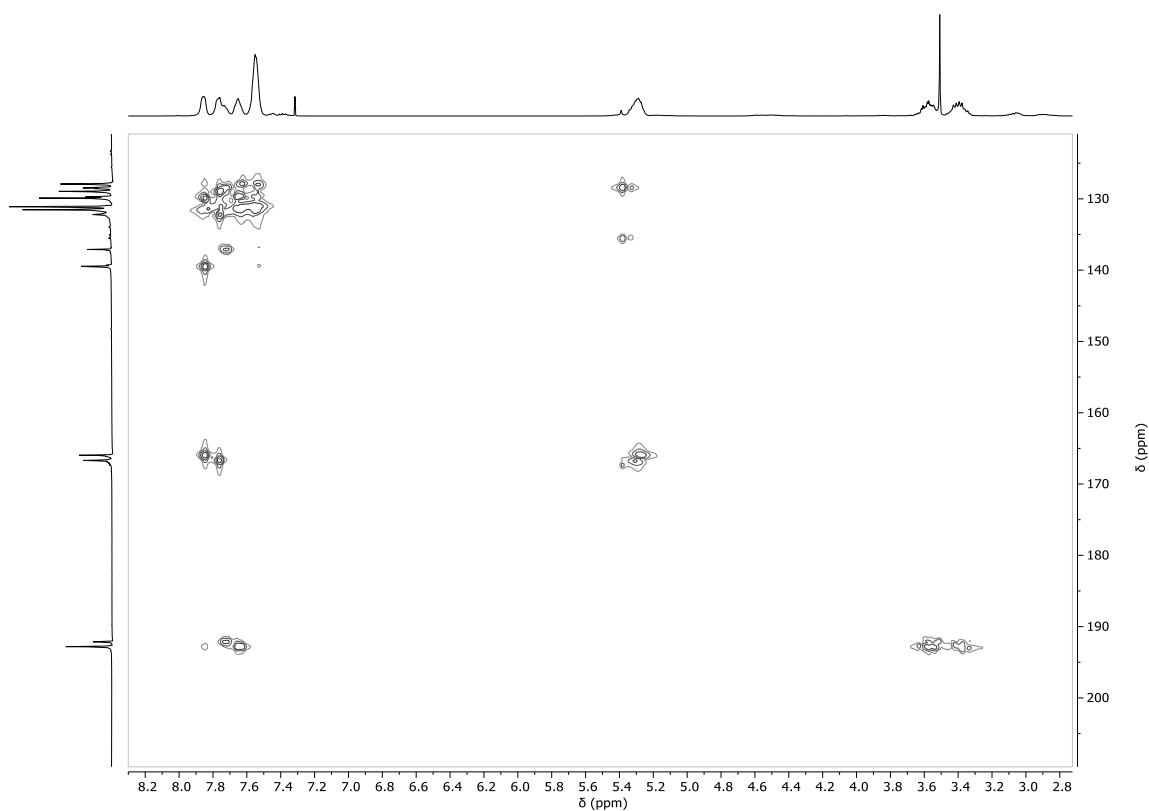


Figure S 19: ^1H - ^{13}C HMBC NMR spectrum (CDCl_3 , 25°C) of copolymer corresponding to table 1, run #15.

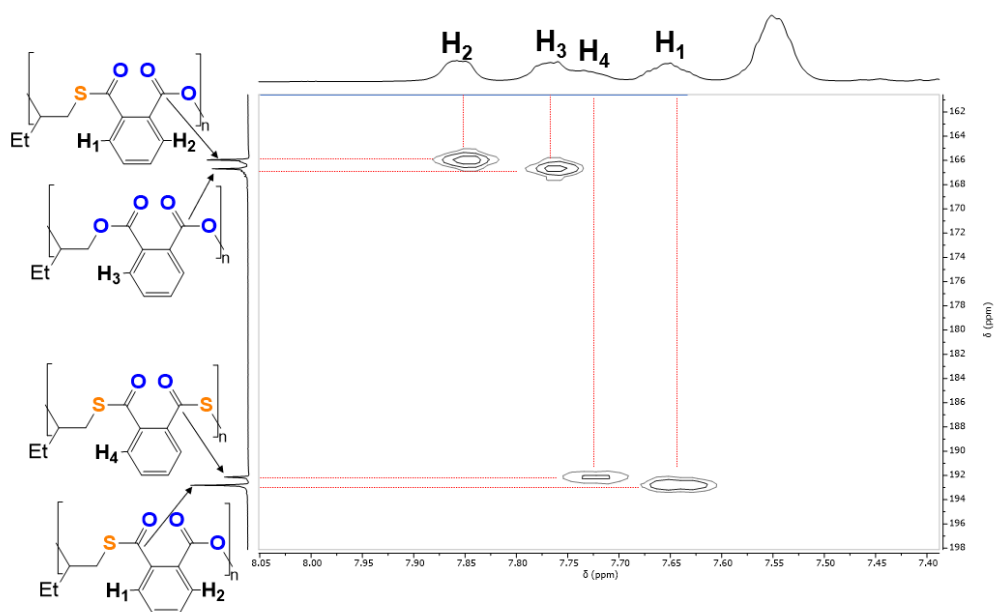


Figure S 20: Zoom into the ^1H - ^{13}C HMBC NMR spectrum (CDCl_3 , 25°C) of copolymer corresponding to table 1, run #15.

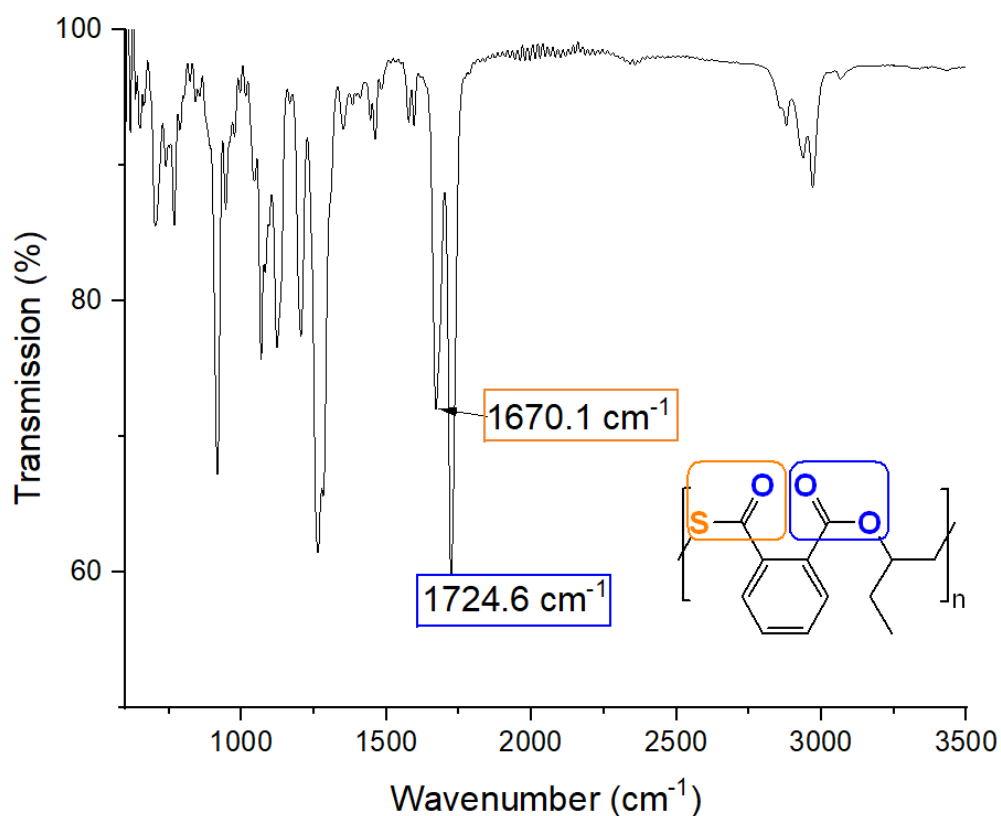


Figure S 21: FT ATR-IR spectrum of copolymer corresponding to table 1, run #9.

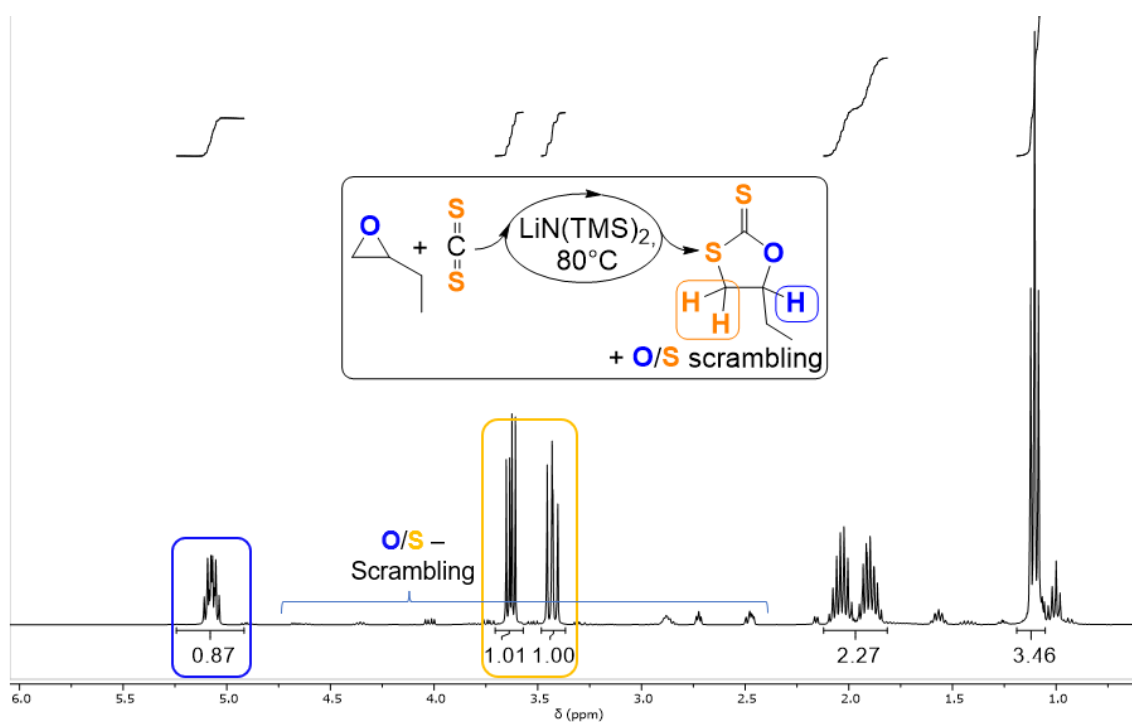


Figure S 22: ^1H NMR spectrum (400 MHz, CDCl_3 , 25°C) of reaction mixture produced according to Table 1, #14.

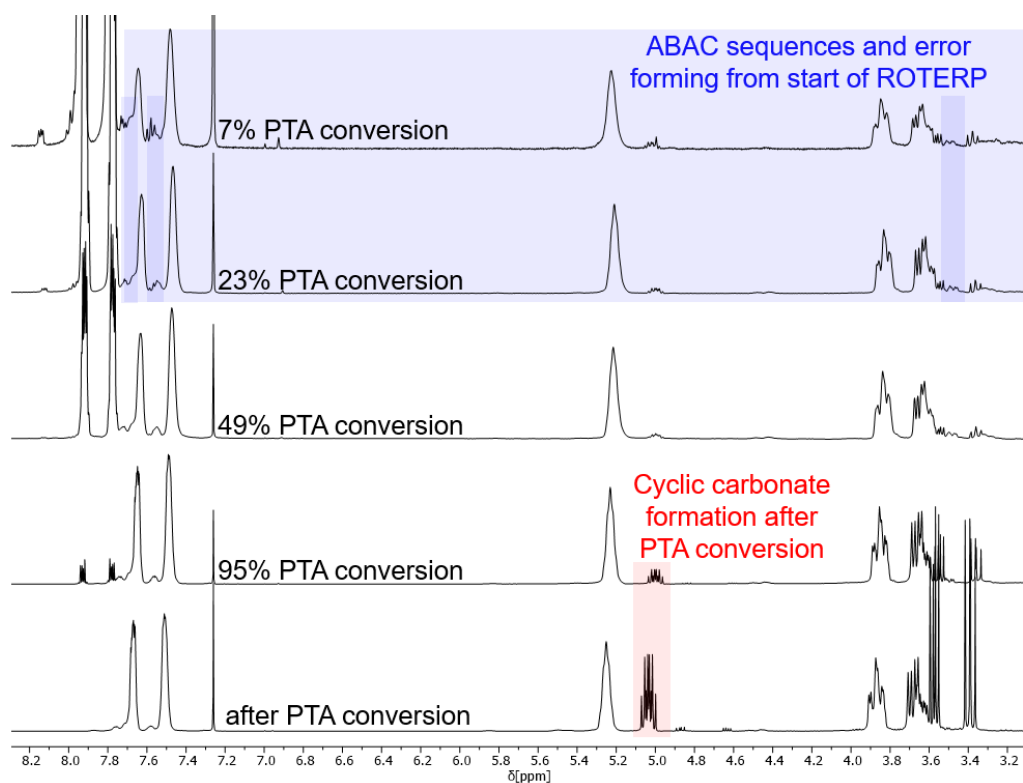


Figure S 23: ¹H NMR spectrum (400 MHz, CDCl₃, 25°C) of aliquots removed at different stages of ROTERP corresponding to table 1, run #9.

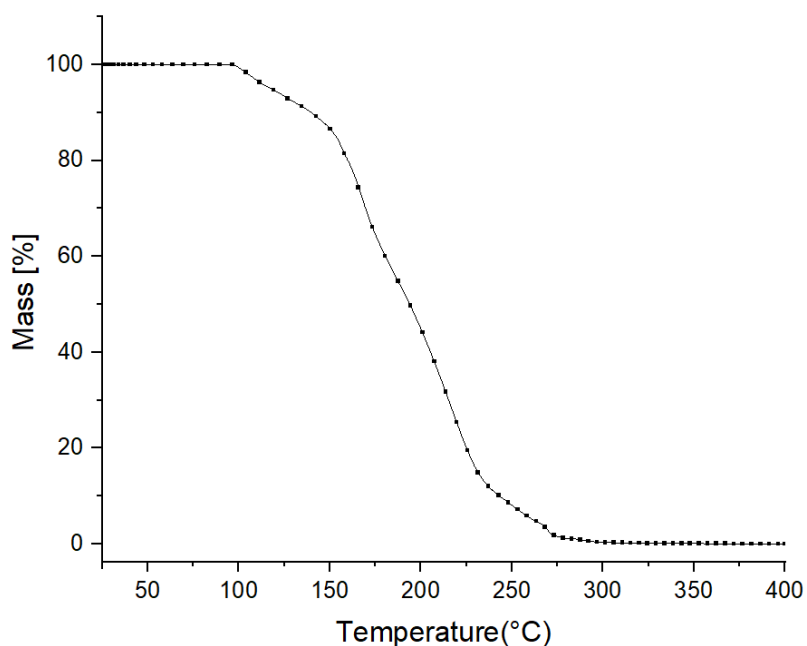


Figure S 24: TGA of CS₂/PO copolymer reported in this study obtained from the reaction of 1 LiHMDS: 500 PO : 1000 CS₂ at 25°C for 16h.

Section S4: SEC traces

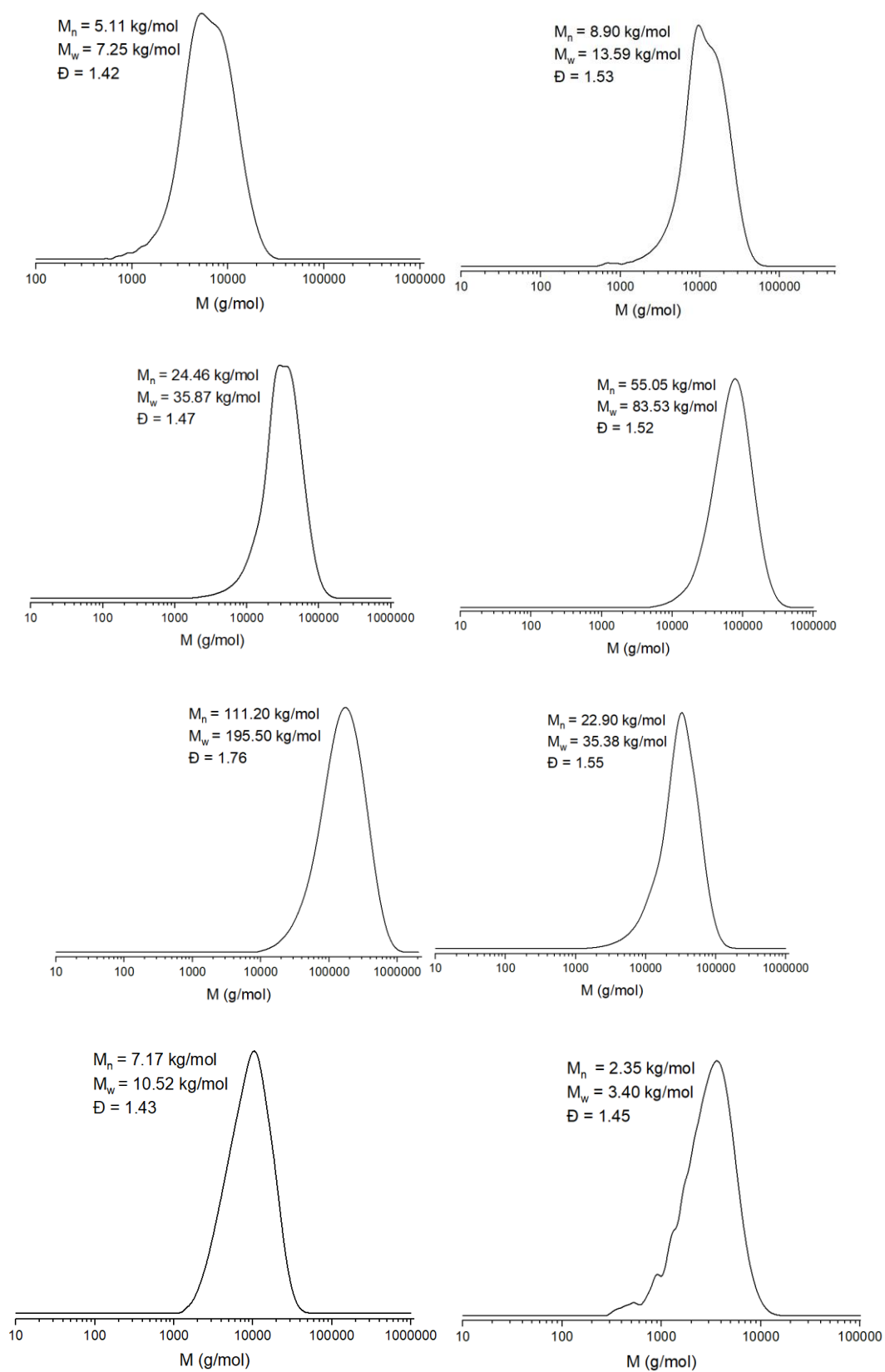


Figure S 25: SEC traces of polymers reported in this study.

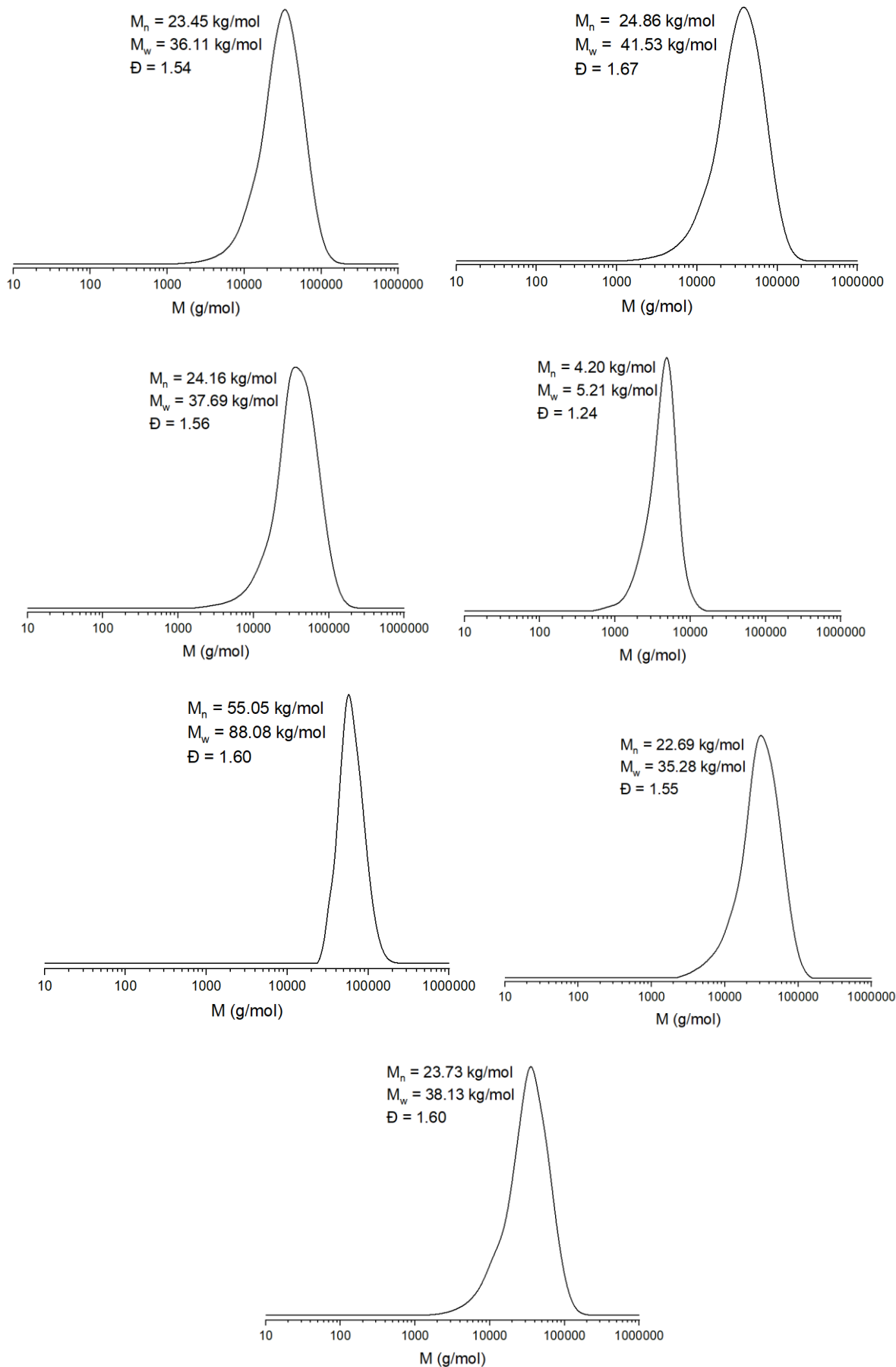


Figure S 26: SEC traces of polymers reported in this study.

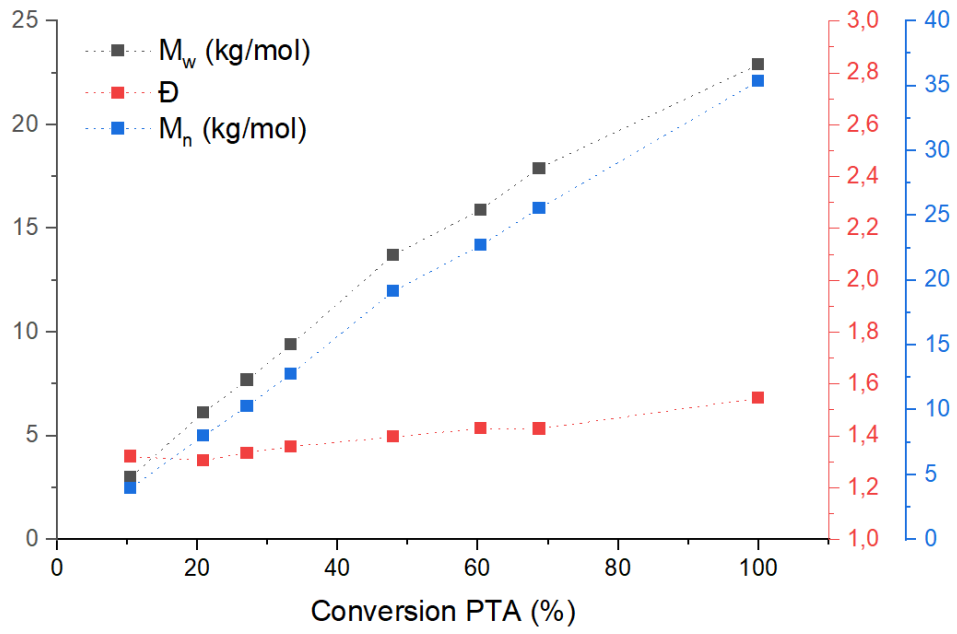
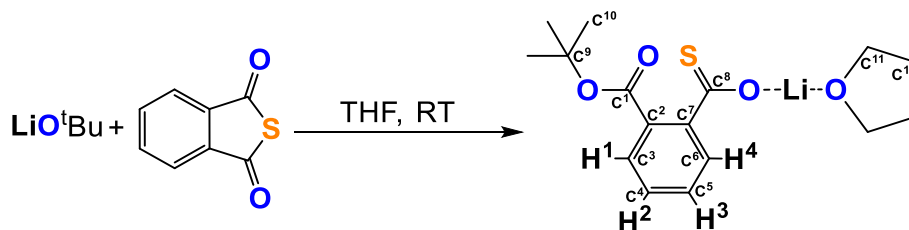


Figure S 27: Development of molecular masses and polydispersity of terpolymer corresponding to table 1, run #9.

Section S5: Synthesis, characterisation and reactivity of model MTC



Synthesis of MTC-THF: Inside an Argon filled glovebox, phthalic thioanhydride (164.2 mg, 1.00 mmol) and LiOtBu (80.0 mg, 1.00 mmol) were loaded into an oven dried Schenk fask, brought outside the glovebox and connected to an Schlenkline. Dry THF (25mL) was added and the mixture was stirred overnight giving an orange solution. All volatiles were removed in vacuum yielding **MTC-THF** as a yellow solid (300.0 mg, 0.95 mmol, 95%). XRD quality crystals were grown by layering a saturated THF solution with Pentane.

^1H NMR (400 MHz, d_8 -THF, 25°C); δ (ppm): 7.77 (dd, $J = 7.5, 1.1$ Hz, 1H, H^4), 7.35 (dd, $J = 7.5, 1.1$ Hz, 1H, H^1), 7.25 (td, $J = 7.5, 1.4$ Hz, 1H, H^2), 7.16 (td, $J = 7.5, 1.3$ Hz, 1H, H^3), 3.65 – 3.53 (m, 4H, THF), 1.86 – 1.71 (m, 4H, THF), 1.52 (s, 6H, tBu).

$^{13}\text{C}\{^1\text{H}\}$ NMR (101 MHz, d_8 -THF, 25°C); δ (ppm): 218.63 (C8), 169.33 (C1), 149.04 (C7), 131.31 (C2), 129.61 (C3), 129.47 (C5), 128.06 (C4), 127.24 (C6), 80.81 (C11), 68.02 (C9), 28.08 (C12), 26.13 (C10).

^7Li NMR (156 MHz, d_8 -THF, 25°C); δ (ppm): 0.63.

FTIR [cm^{-1}]: 1685.1 (Ester $\text{C}=\text{O}$), 1450.8 (Thiocarboxylate $\text{C}=\text{O}$)

HRESI-MS (negative mode): $m/z =$ calculated $[\text{M} - \text{Li}]^-$ 237.0585. Found 237.0650

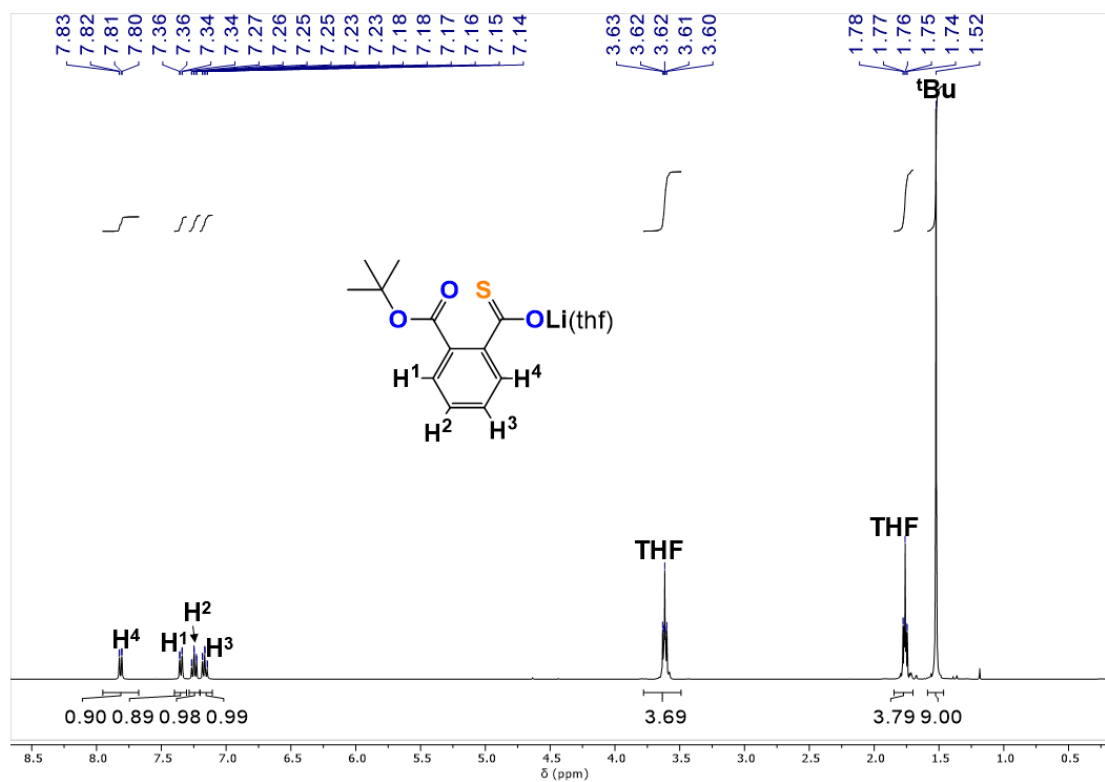


Figure S 28: ¹H NMR spectrum (400 MHz, d₈-THF, 25°C) of MTC-THF.

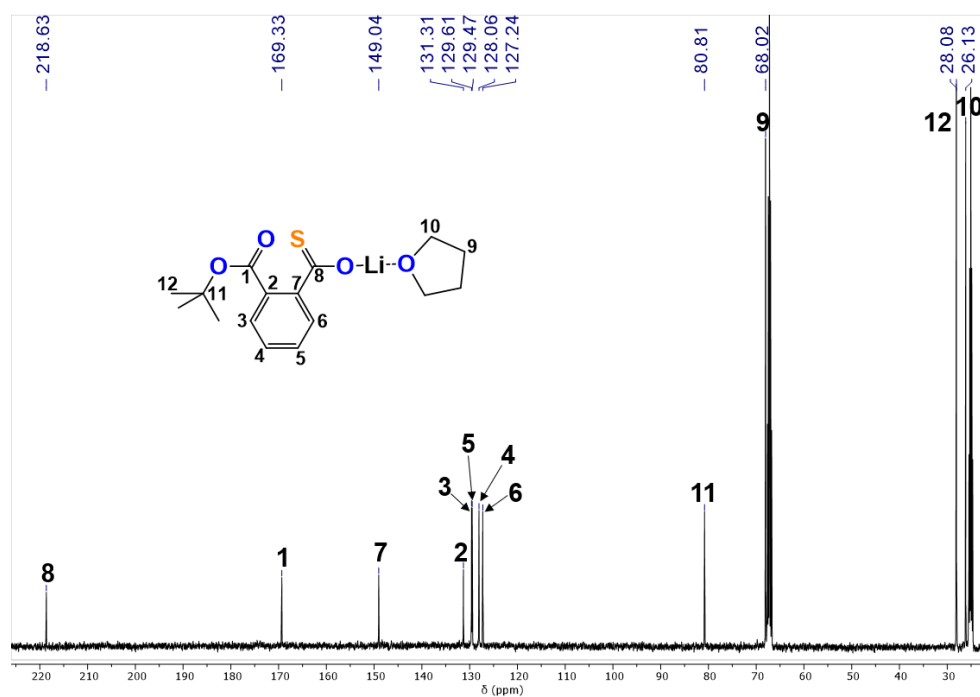


Figure S 29: ¹³C{¹H} NMR spectrum (101 MHz, d₈-THF, 25°C) of MTC.

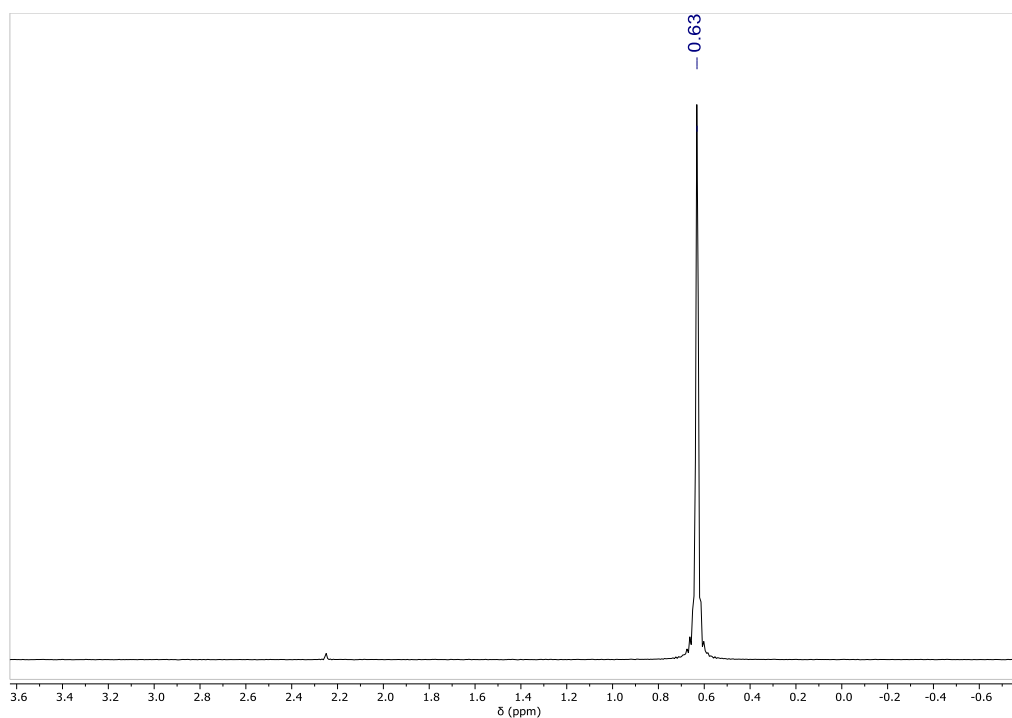


Figure S 30: ^7Li NMR spectrum (194 MHz, d_8 -THF, 25°C) of **MTC**. Signal at 2.25 ppm corresponds to internal LiSO_3CF_3 standard.

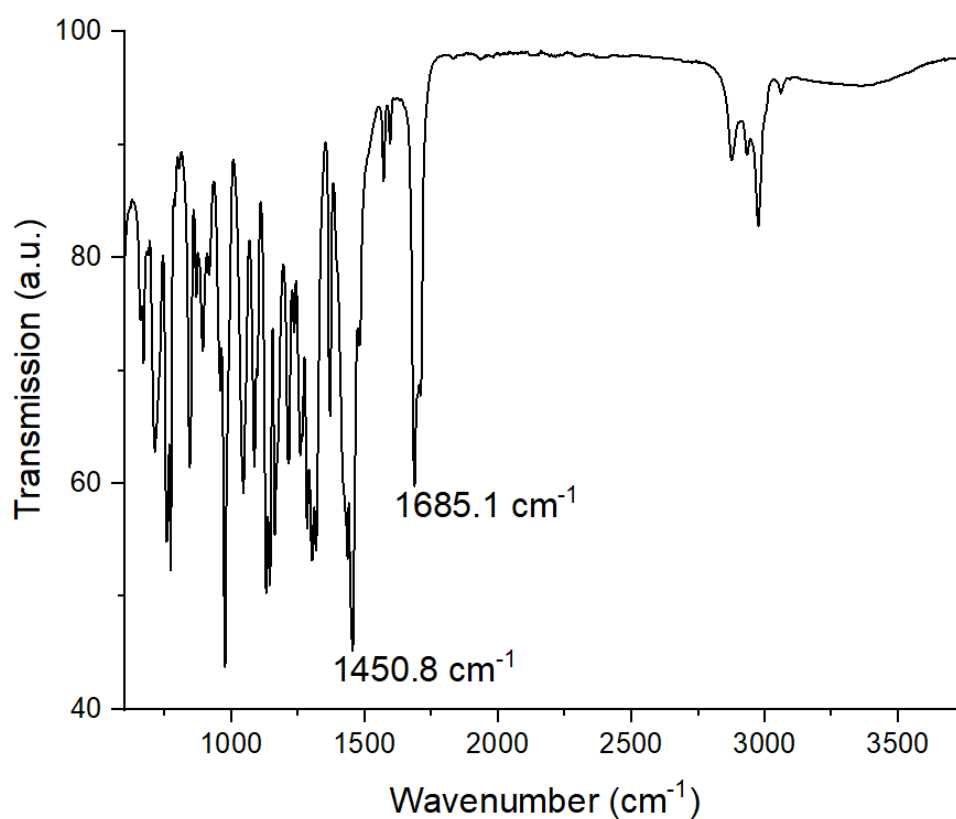
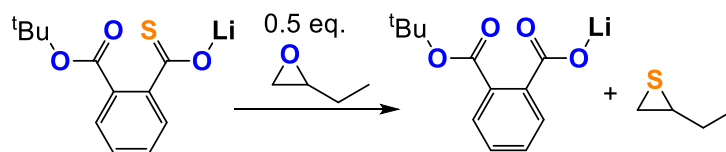


Figure S 31: Solid state FT-ATIR spectrum of **MTC**.



In an oven dried J. Youngs NMR Tube **MTC**·THF (50.0 mg, 0.16 mmol, 1 eq.) dissolved in d_8 -THF (0.6 mL) and BO (7.0 μ L, 0.08 mmol, 0.5 equiv.) was let react for 10 min and analysed by NMR. The mixture was then let react for another 2h and analysed by NMR. Longer reaction times or more equivalents BO result in the appearance of broad signal under disappearance of the thiiran signals presumably due to competitive formation of polythioether.

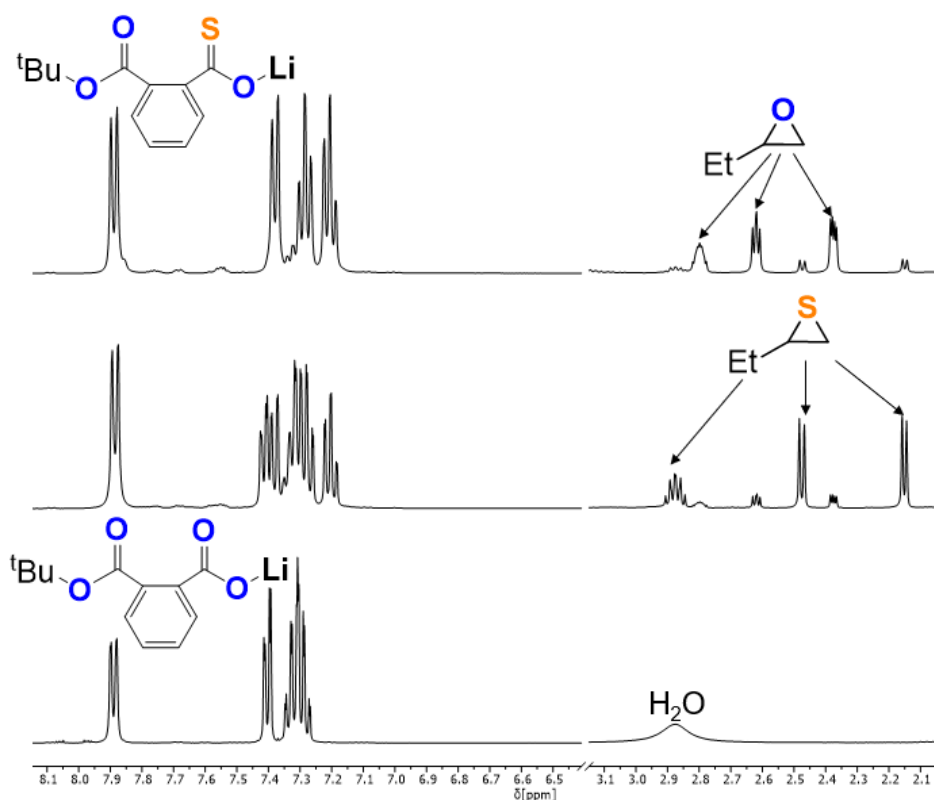
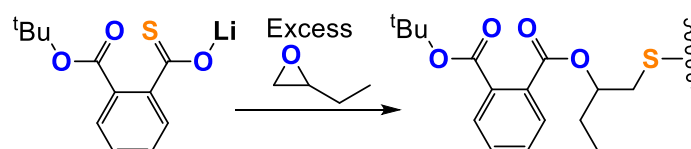


Figure S 32: Overlaid ^1H NMR (400 MHz, d_8 -THF, 25°C) spectra of BO addition to **MTC** (top) 10 min after addition and (middle) 2h after addition and (bottom) carboxylate derivative of **MTC** prepared from 1 eq. LiO^tBu with phthalic anhydride.



BO insertion from MTC: Excess butylene oxide (1mL) was added to solid **MTC**·THF (50mg). The resulting mixture was stirred for 30 min at room temperature before all volatiles were removed in vacuum prior to spectroscopic analysis.

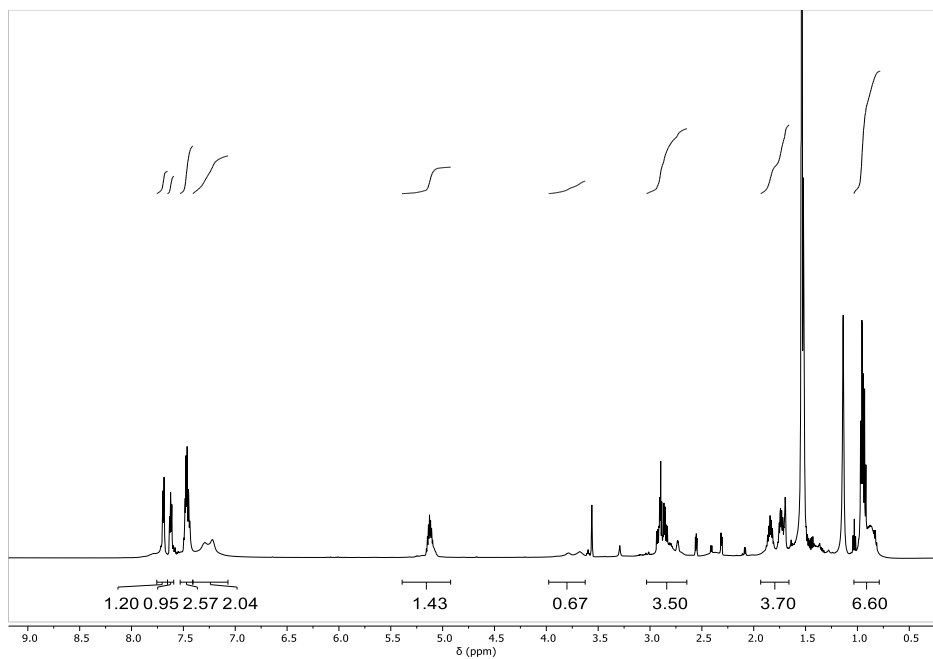


Figure S 33: ^1H NMR spectrum (400 MHz, d_8 -THF, 25°C) of BO insertion products of **MTC**.

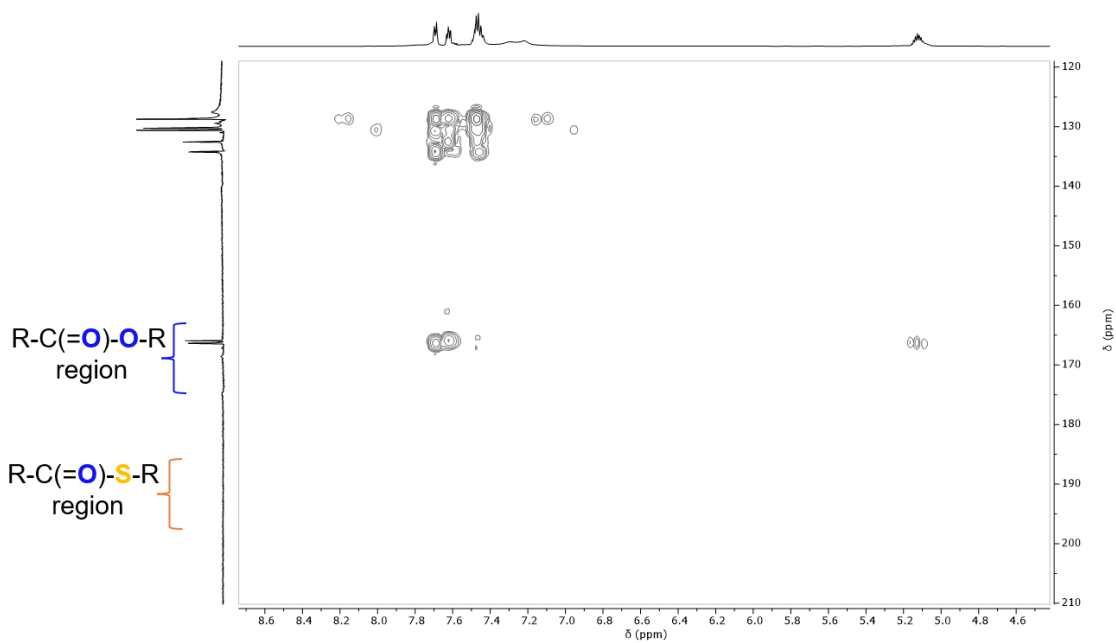


Figure S 34: Zoom into the carbonyl region of the ^1H - ^{13}C HMBC NMR spectrum (d_8 -THF, 25°C) of BO insertion of **MTC**.

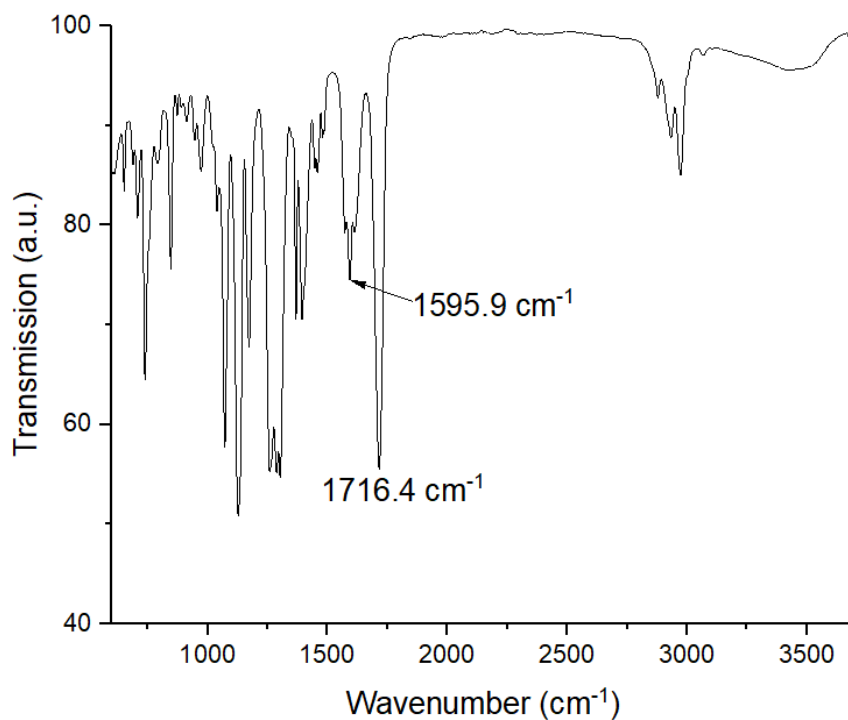


Figure S 35: Solid state FTIR spectrum of BO insertion of **MTC**.

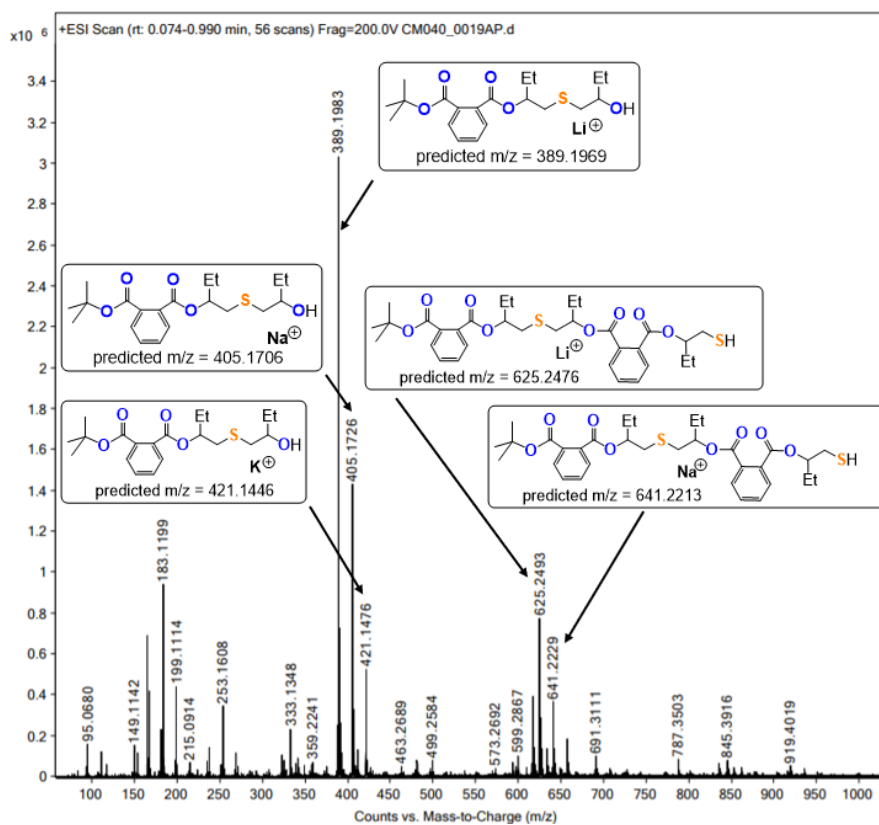


Figure S 36: Positive Mode HR-ESI MS of BO insertion products of **MTC**.

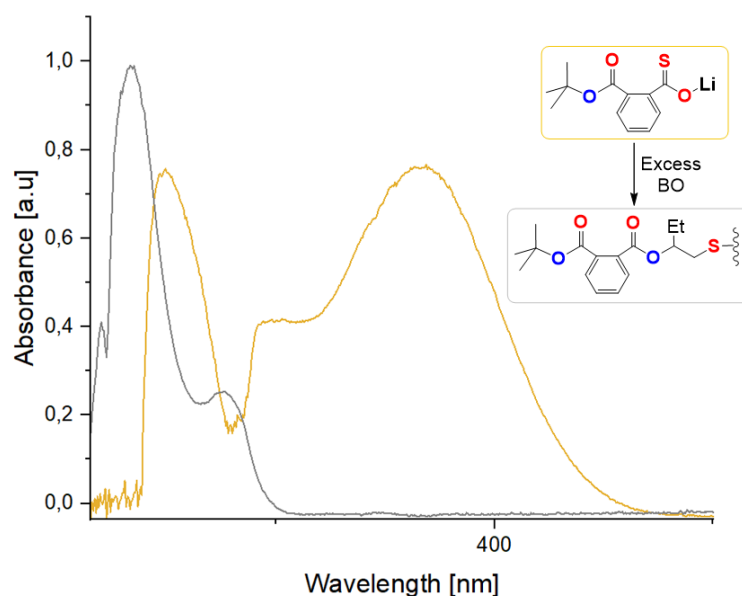


Figure S 37: UVVIS spectra before and after BO insertion of **MTC** in THF.

Reaction between MTC and BO in presence of CS₂: In an oven dried J. Youngs NMR Tube **MTC**-THF (50.0 mg, 0.16 mmol, 1 eq.) dissolved in d₈-THF (0.4 mL) and CS₂ (0.4 mL, 6.6 mmol, 42 equiv.) and BO (7.0 μL, 0.08 mmol, 0.5 equiv.) was added. The mixture was let react for 5 min and analysed by NMR.

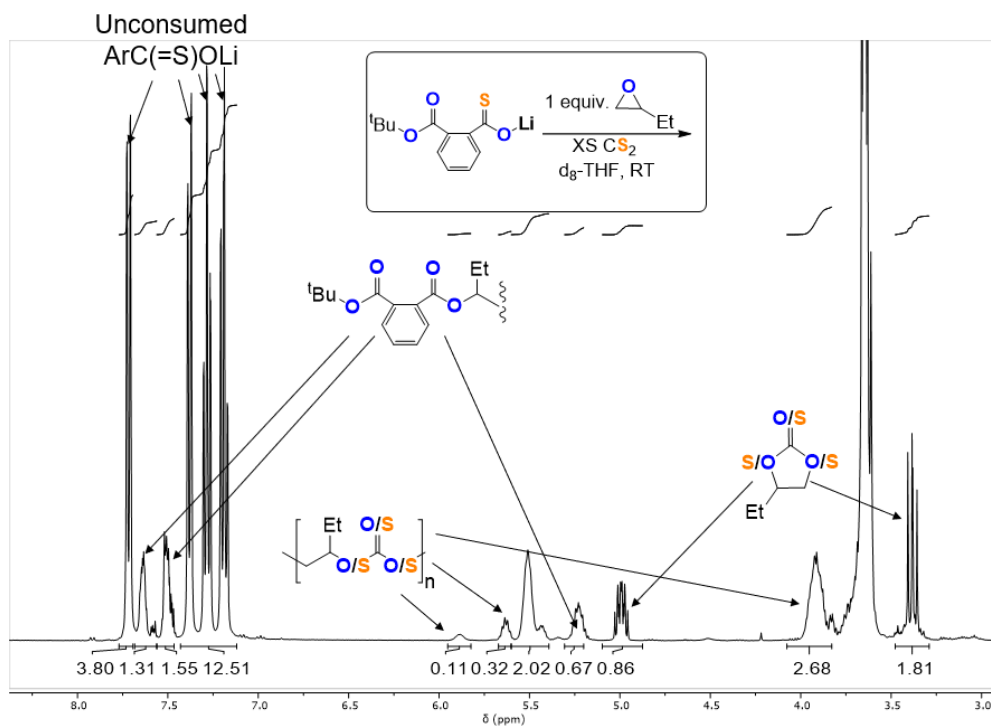


Figure S 38: ¹H NMR spectrum (400 MHz, d₈-THF, 25°C) of product mixture produced from the reaction of **MTC** with 1 eq. BO in presence of excess CS₂.

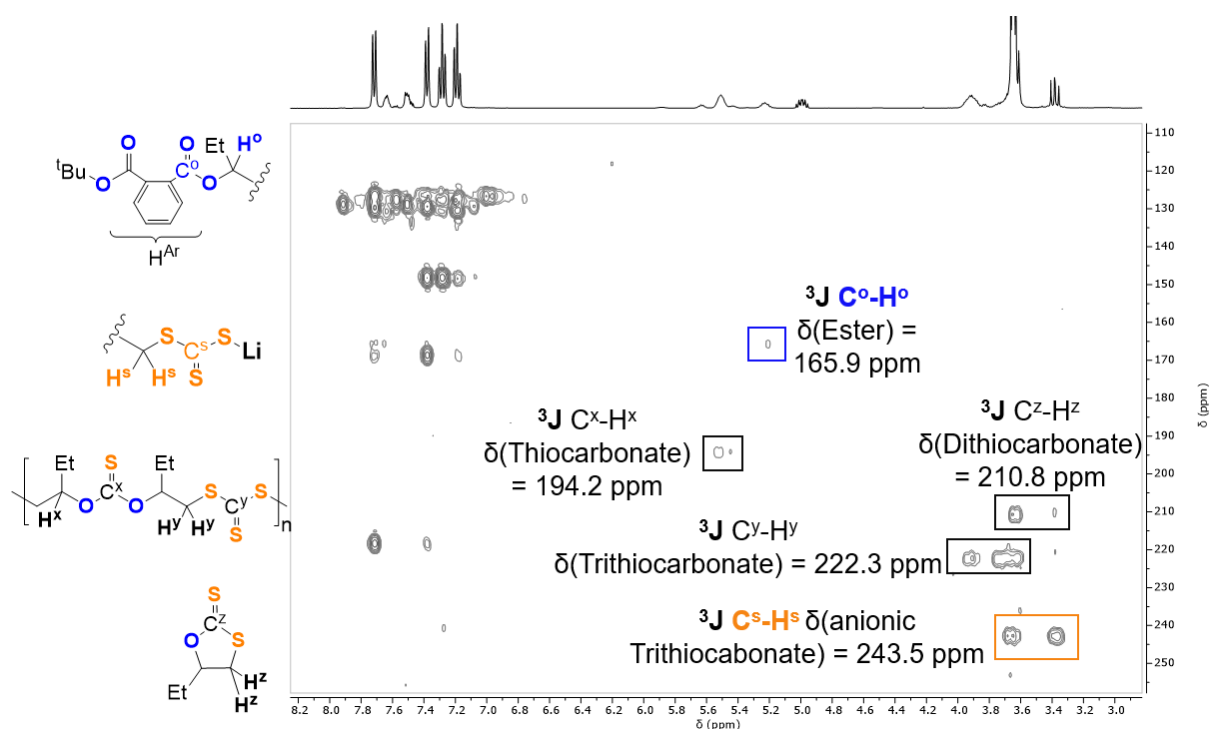
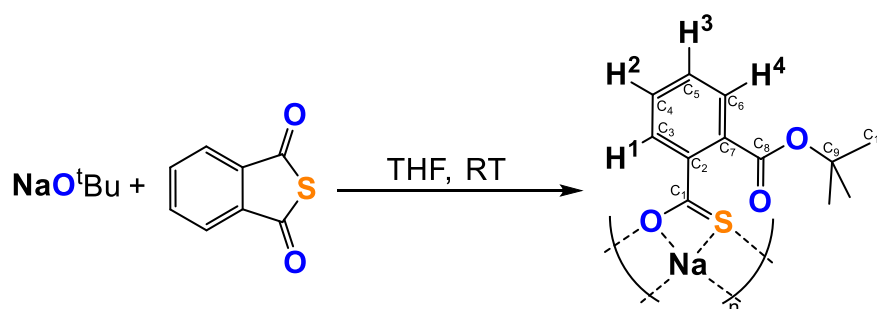


Figure S 39: ^1H - ^{13}C HMBC NMR spectrum (d₈-THF, 25°C) of product mixture produced from the reaction of **MTC** with 1 eq. BO in presence of excess CS₂.



Synthesis of **MTC^{Na}·0.75THF:** Inside an Argon filled glovebox, phthalic thioanhydride (164.2 mg, 1.00 mmol) and NaOtBu (96.0 mg, 1.00 mmol) were loaded into an oven-dried Schlenk flask, brought outside the glovebox and connected to a Schlenkline. Dry THF (25mL) was added, and the mixture was stirred overnight giving an orange suspension. All volatiles were removed in vacuum yielding **MTC**^{Na} as a orange solid (298.3 mg, 0.95 mmol, 95%). XRD quality crystals were grown by layering the crude reaction mixture with pentane.

^1H NMR (400 MHz, d₈-THF, 25°C); δ (ppm): 7.83 (d, $J = 7.5$ Hz, 1H, H-1), 7.35 – 7.14 (m, 4H, H-2/H-3/H-4), 3.82 – 3.37 (m, THF), 2.01 – 1.61 (m, THF), 1.48 (s, 9H, ^tBu).

Due to the insolubility of **MTC**^{Na}, ^{13}C data was obtained via ^1H - ^{13}C HMBC NMR spectroscopy.

$^{13}\text{C}\{^1\text{H}\}$ NMR (101 MHz, $\text{d}_8\text{-THF}$, 25°C); $\delta(\text{ppm})$: 209.92 (C1), 169.52 (C8), 148.29 (C2), 131.29 (C7), 129.45 (C6), 129.00 (C4), 127.41 (C5), 127.00 (C2), 80.28 (C9), 28.34 (C10)

FTIR [cm^{-1}]: 1684.0 (Ester C=O), 1451.6 (Thiocarboxylate C=O)

HRESI-MS (negative mode): m/z = calculated $[\text{M} - \text{Na}]^-$ 237.0585. Found 237.0545

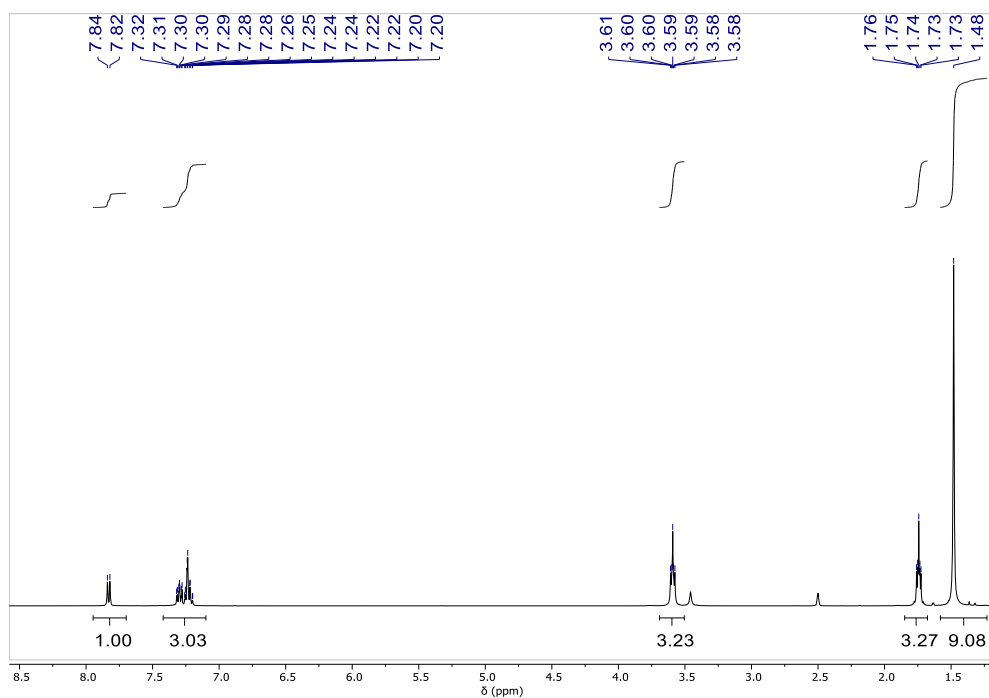


Figure S 40: ^1H NMR spectrum (400 MHz, $\text{d}_6\text{-DMSO}$, 25°C) of $\text{MTC}^{\text{Na}}\cdot 0.75\text{THF}$.

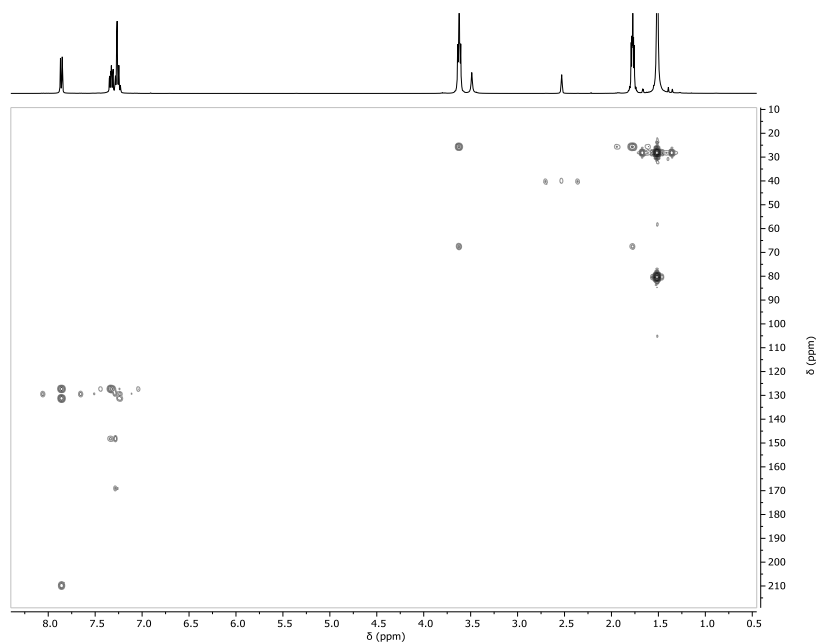


Figure S 41: $^1\text{H} - ^{13}\text{C}$ HMBC NMR spectrum (126 MHz, CDCl_3 , 25°C) of $\text{MTC}^{\text{Na}}\cdot 0.75\text{THF}$.

Reaction between MTC^{Na} and BO in presence of CS₂: In an oven dried J. Youngs NMR Tube **MTC**-0.75THF (50.3 mg, 0.16 mmol, 1 eq.) dissolved in d₈-THF (0.4 mL) and CS₂ (0.4 mL, 6.6 mmol, 42 equiv.) and BO (7.0 μL, 0.08 mmol, 0.5 equiv.) was added. The mixture was let react for 16 h and analysed by NMR.

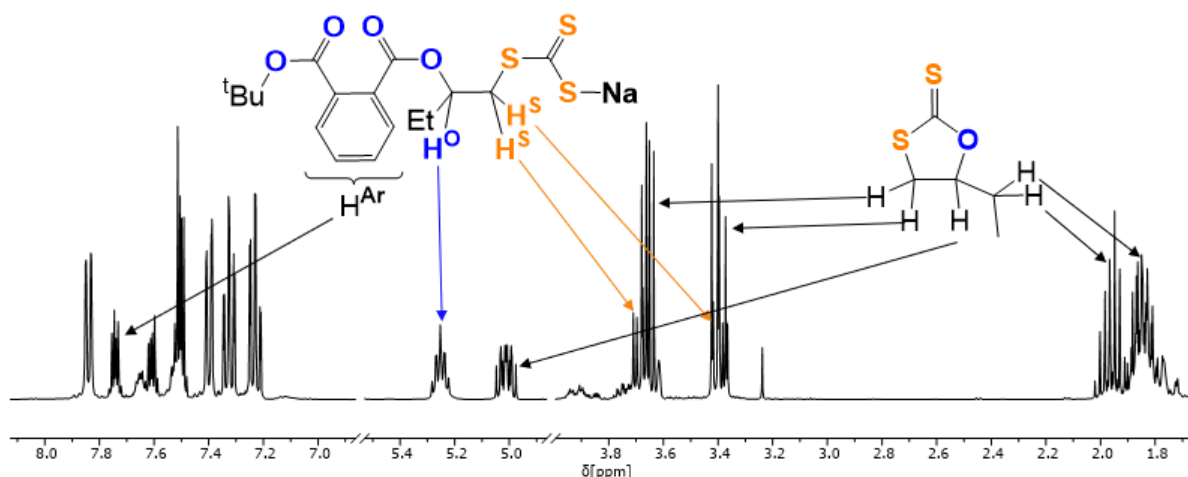
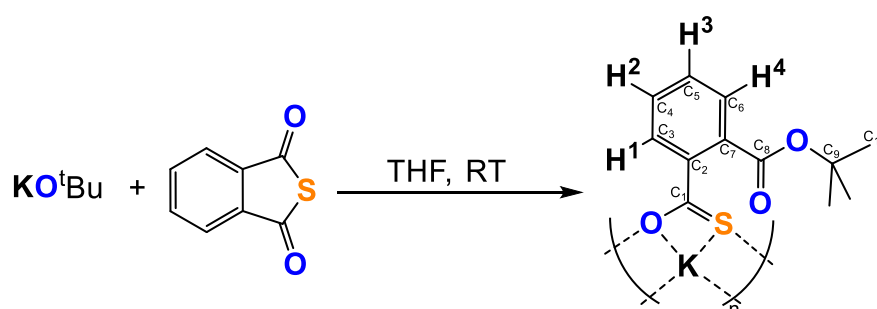


Figure S 42: ¹H NMR spectrum (400 MHz, d₈-THF, 25°C) of product mixture product from the stoichiometric reaction of



Synthesis of MTC^K: Inside an Argon filled glovebox, phthalic thioanhydride (164.2 mg, 1.00 mmol) and KO^tBu (112.2 mg, 1.00 mmol) were loaded into an oven-dried Schenk fask, brought outside the glovebox and connected to an Schlenkline. Dry THF (25mL) was added and the mixture was stirred overnight giving an orange suspension. All volatiles were removed in vacuum yielding **MTC^K** as a orange solid (262.6 mg, 0.95 mmol, 95%). XRD quality crystals were grown by layering a crude reaction mixture with Pentane.

¹H NMR (400 MHz, d₈-THF, 25°C); δ(ppm): δ 7.79 (ddd, J = 7.7, 1.2, 0.6 Hz, 1H, H¹), 7.27 (ddd, J = 7.7, 6.4, 2.3 Hz, 1H, H²), 7.23 – 7.15 (m, 2H, H^{3/4}), 1.46 (s, 9H, ^tBu).

Due to the insolubility of **MTC^K**, ¹³C data was obtained via ¹H-¹³C HMBC NMR spectroscopy.

$^{13}\text{C}\{^1\text{H}\}$ NMR (101 MHz, $\text{d}_8\text{-THF}$, 25°C); $\delta(\text{ppm})$: 208.10 (C1), 169.31 (C8), 148.84 (C2), 131.10 (C7), 129.24 (C6), 129.00 (C4), 127.23 (C5), 126.96 (C2), 81.50 (C9), 28.90 (C10)

FTIR [cm^{-1}]: 1684.5 (Ester C=O), 1451.9 (Thiocarboxylate C=O)

HRESI-MS (negative mode): m/z = calculated $[\text{M} - \text{K}]^-$ 237.0585. Found 237.0572

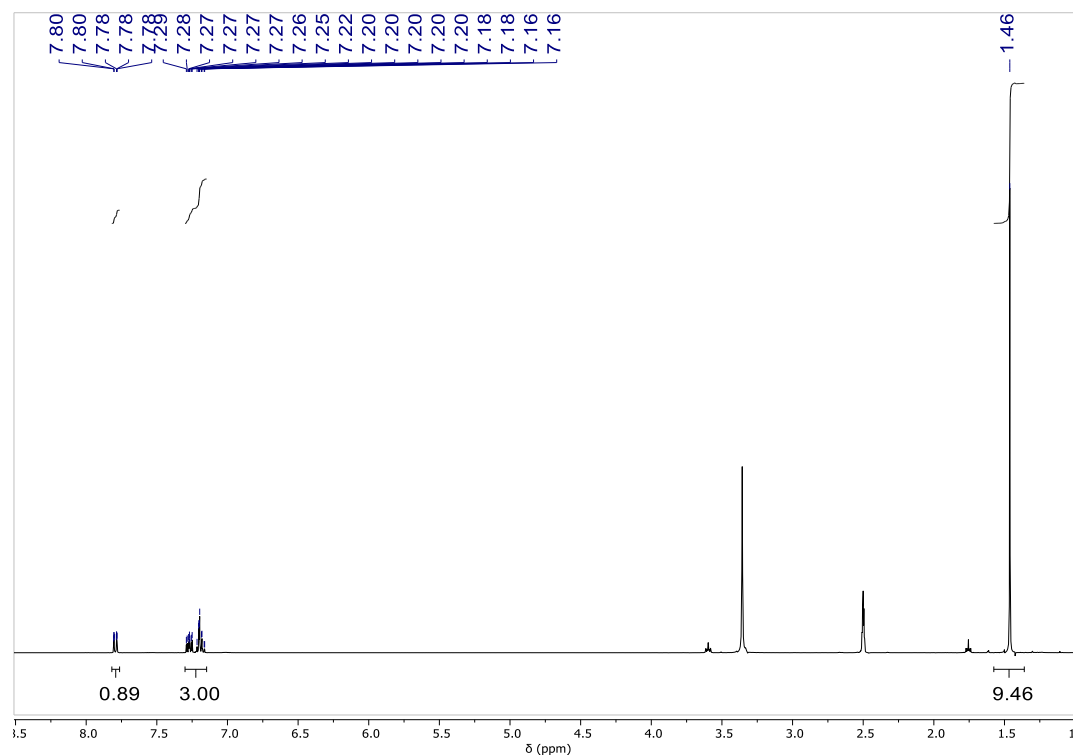


Figure S 43: ^1H NMR spectrum (400 MHz, $\text{d}_6\text{-DMSO}$, 25°C) of MTC^{K} .

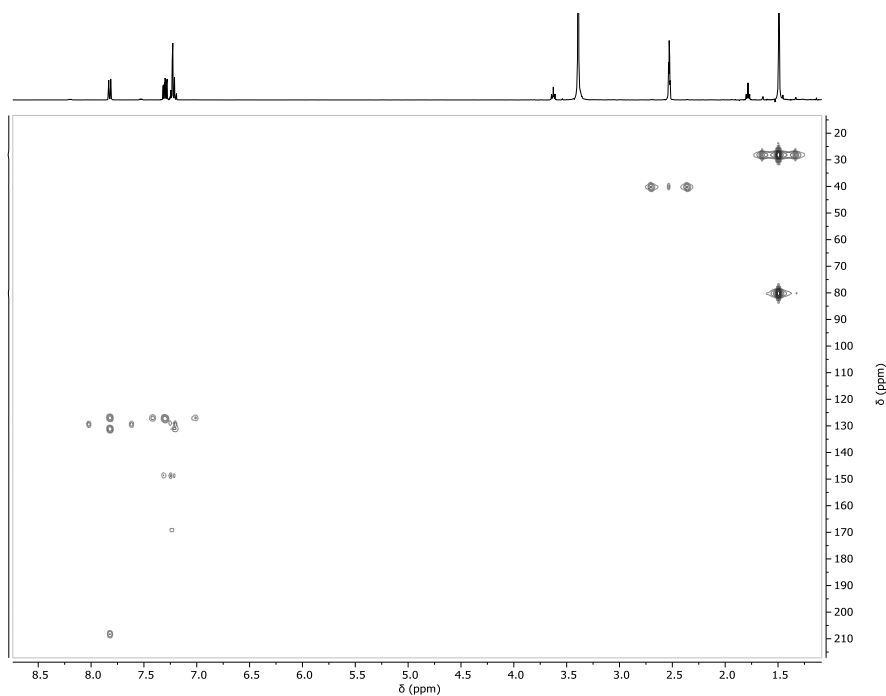


Figure S 44: ^1H - ^{13}C HMBC NMR spectrum (CDCl_3 , 25°C) of **MTC^K**.

Section S6: Switchable Catalysis.

ϵ DL ROP protocol: In an argon-filled glovebox, LiHMDS (6.4 mg, $38.5\ \mu\text{mol}$, 1 equiv.) was dissolved in butylene oxide (1670.0 μl , 1386.9 mg, 19.2 mmol, 500 equiv.) and benzylalcohol (4.0 μl , 4.2 mg, $36.5\ \mu\text{mol}$, 1 equiv.) was added. The resulting mixture was stirred for 1 min and afterwards ϵ -decalactone (ϵ DL) (630.6 μl , 655.5 mg, 3.9 mmol, 100 equiv.) was added. Aliquots were removed at regular time intervals and quenched by addition into CDCl_3 containing benzoic acid (10 mg/ml) which were then analysed by ^1H NMR and SEC.

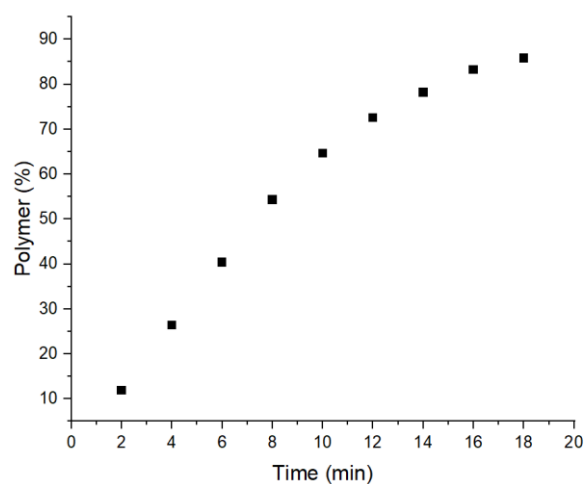


Figure S 45: ϵ DL conversion to PDL polymer versus time plot.

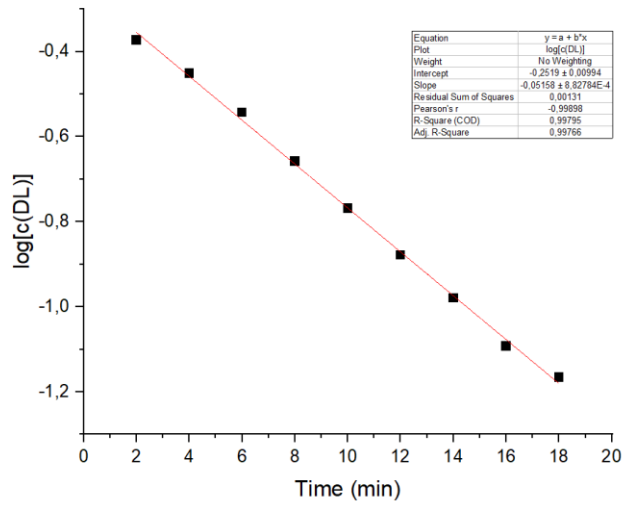


Figure S 46: Logarithmic ϵ DL conversion to PDL polymer versus time plot.

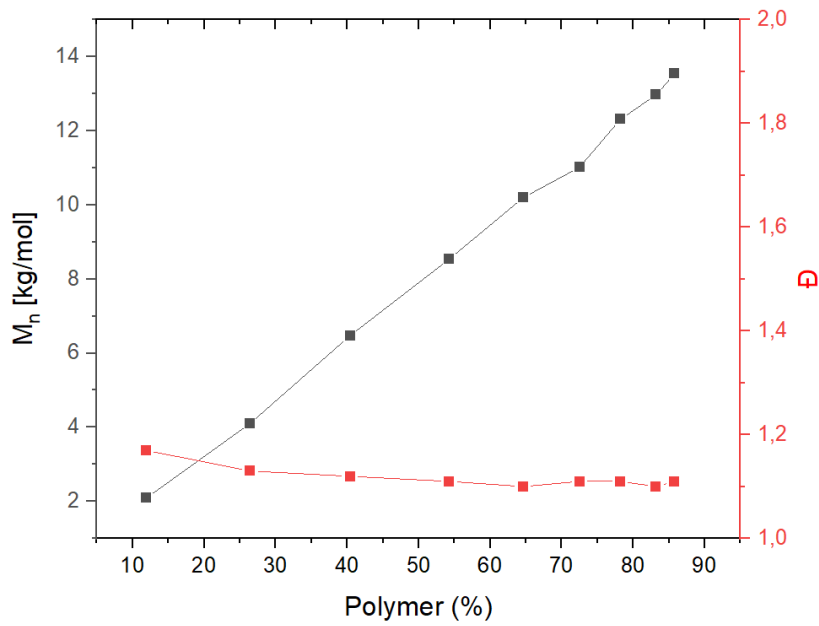


Figure S 47: Plot showing the development of M_n and polydispersity of PDL with respect to ϵ DL conversion.

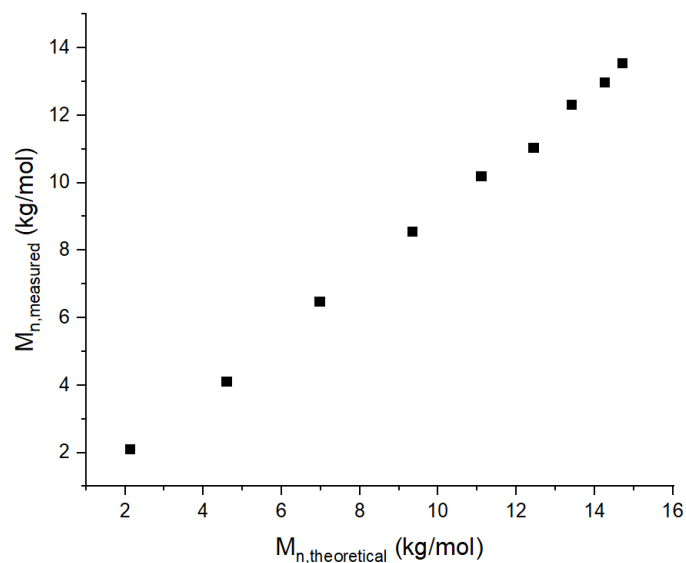


Figure S 48: Correlation of measured and theoretical M_n of PDL.

ϵ DL ROP into PTA/ CS_2 /BO ROTERP switch protocol: In an argon-filled glovebox, LiHMDS (6.4 mg, 38.5 μ mol, 1 equiv.) was dissolved in butylene oxide (835.0 μ l, 693.5 mg, 9.6 mmol, 250 equiv.) and benzylalcohol (4.0 μ l, 4.2 mg, 36.5 μ mol, 1 equiv.) was added. The resulting mixture was stirred for 1 min and afterwards ϵ -decalactone (ϵ DL) (335.3 μ l, 327.3 mg, 19.25 mmol, 50 equiv.) was added and ROP was allowed to occur for 15 min. Afterwards CS_2 (1083.0 μ l, 1364.6 mg, 19.3 mmol) and PTA (442.4 mg, 27.0 mmol, 70 equiv.) were added causing an immediate yellow discolouration of the mixture which was then allowed to react for 30 min at 80°C. The polymer was isolated by two consecutive precipitations from DCM/MeOH, followed by isolation by filtration and drying in a vacuum oven set to 60°C overnight.

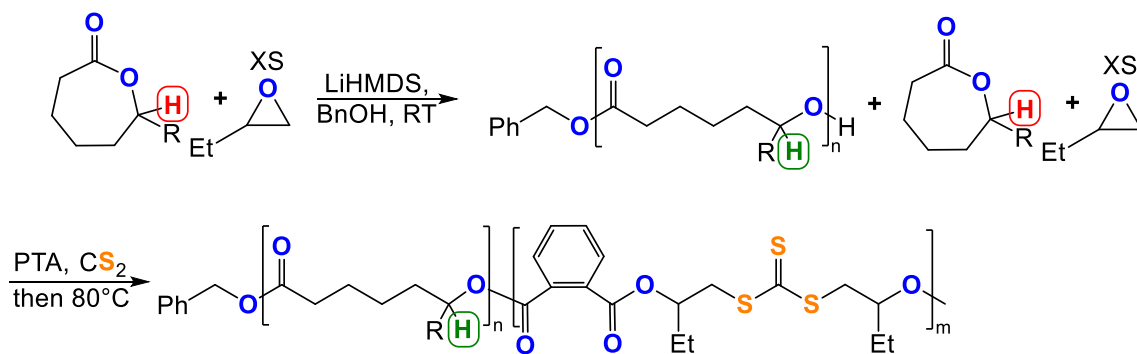


Figure S 49: Schematic showing ϵ DL ROP to PTA/ CS_2 /BO ROTERP switchable catalysis.

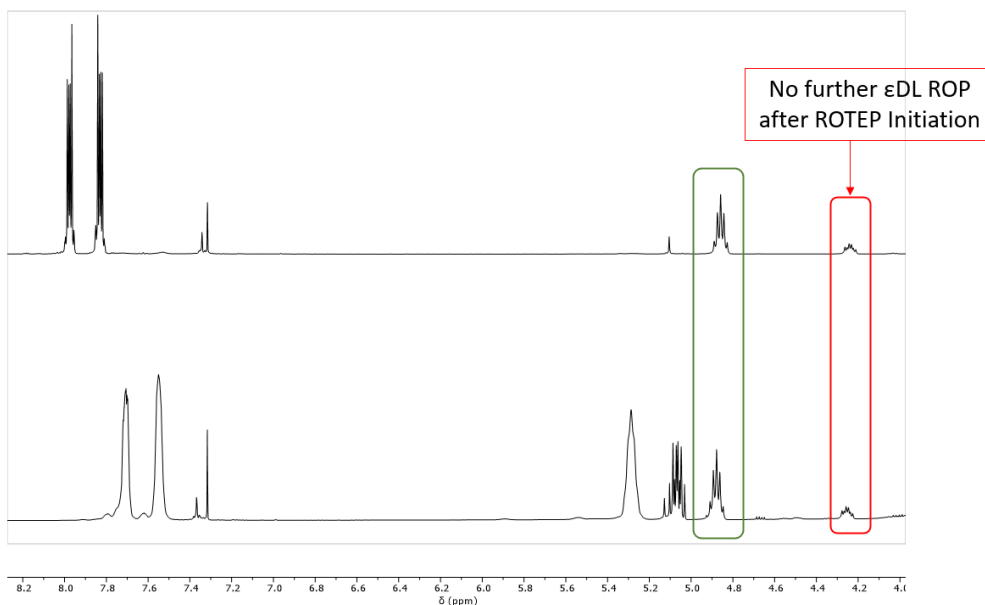


Figure S 50a: ¹H NMR spectra (400 MHz, CDCl₃, 25°C) of aliquots removed before and after ROTERP phase of switchable catalysis showing that no further ROP occurs after ROTERP initiation.

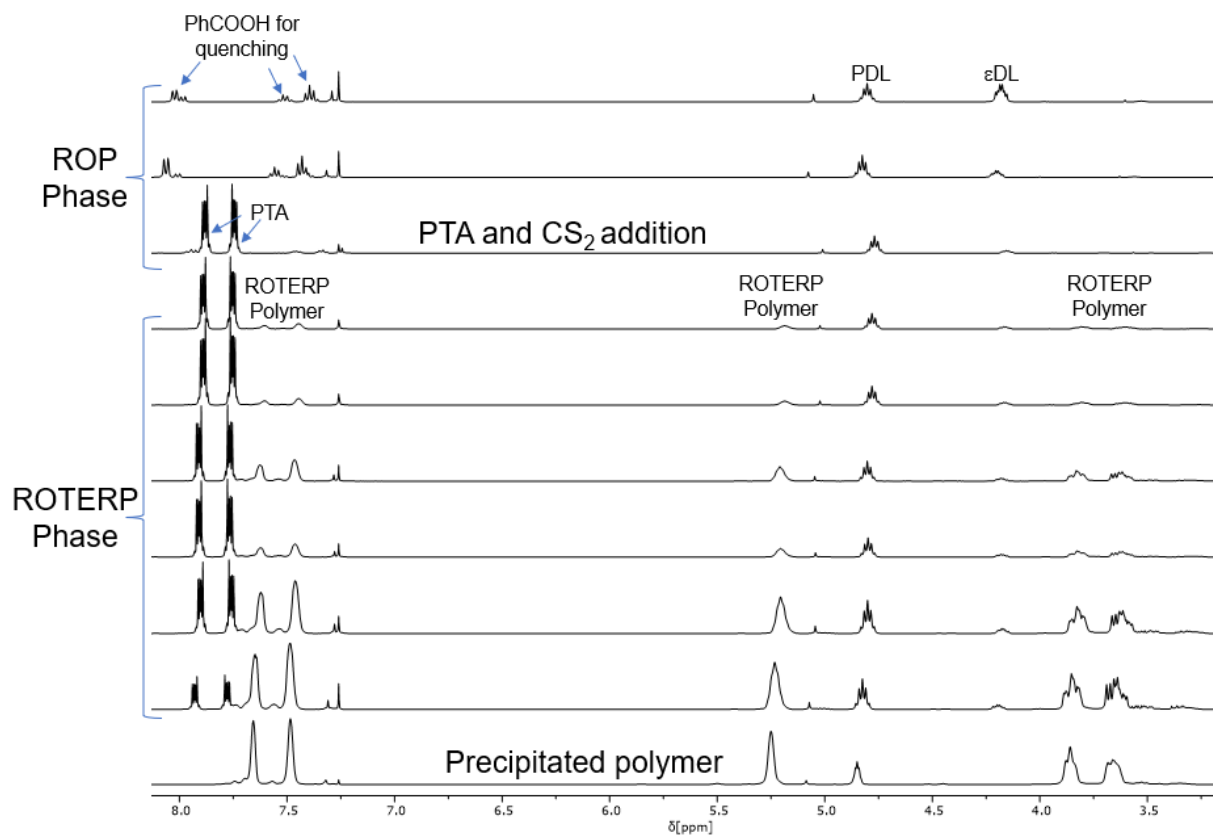


Figure S 51b: ¹H NMR spectra (400 MHz, CDCl₃, 25°C) of aliquots removed throughout ROP and ROTERP phase of switchable catalysis.

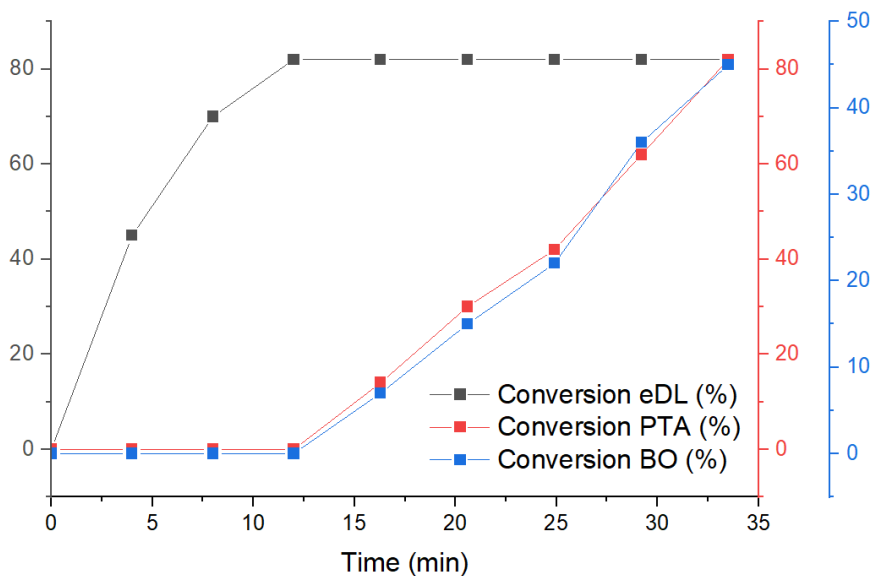


Figure S 52c: Conversion versus time plot (by integration of the ^1H NMR spectra) of switchable catalysis corresponding to Figure S 50b. Note that aliquot removal in the ROP phase results in the final BO conversion deviating from theoretical 40%.

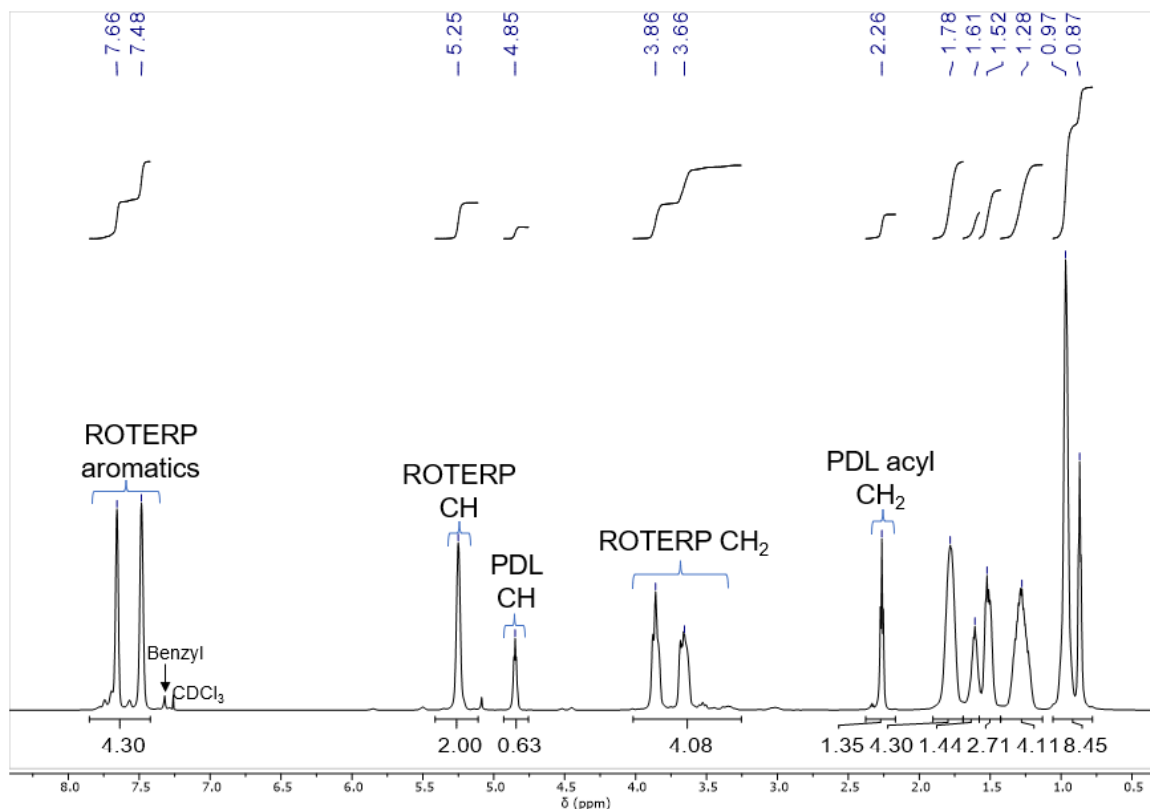


Figure S 53: ^1H NMR spectrum (400 MHz, CDCl_3 , 25°C) of ϵDL ROP to PTA/ CS_2 /BO ROTERP polymer. CH_x labels refer to protons adjacent to heteroatoms.

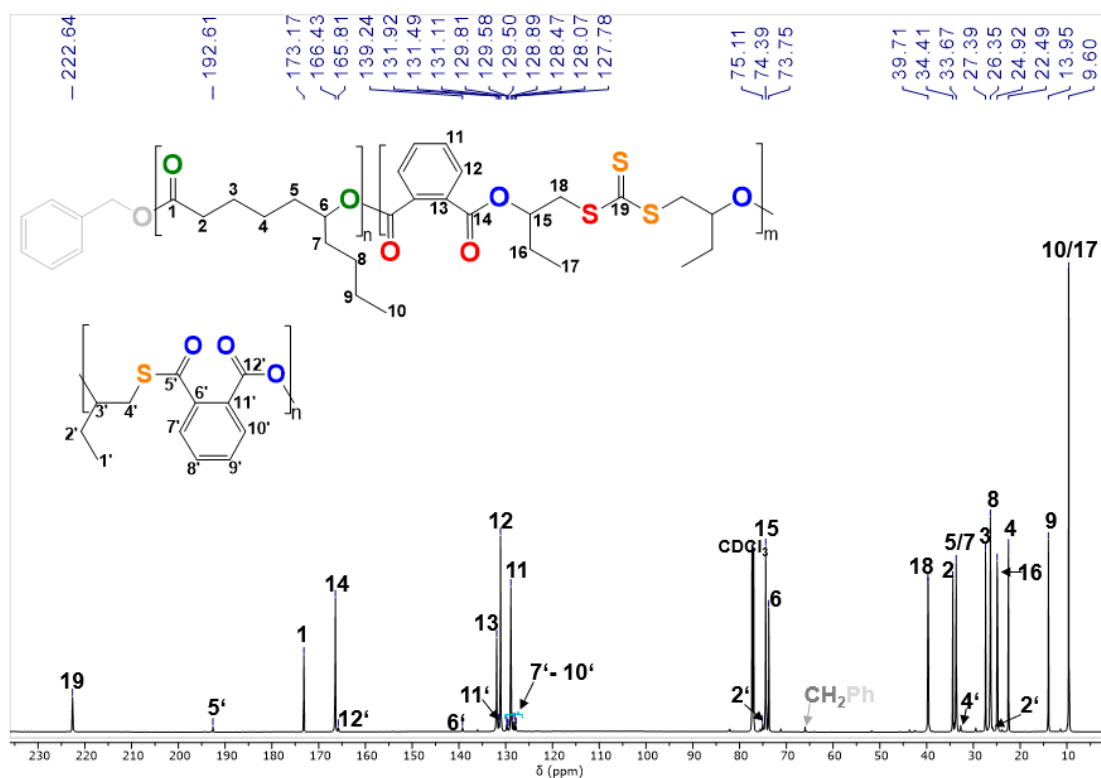


Figure S 54: $^{13}\text{C}\{^1\text{H}\}$ NMR spectrum (126 MHz, CDCl_3 , 25°C) of ϵ DL ROP to PTA/ CS_2 /BO ROTERP polymer.

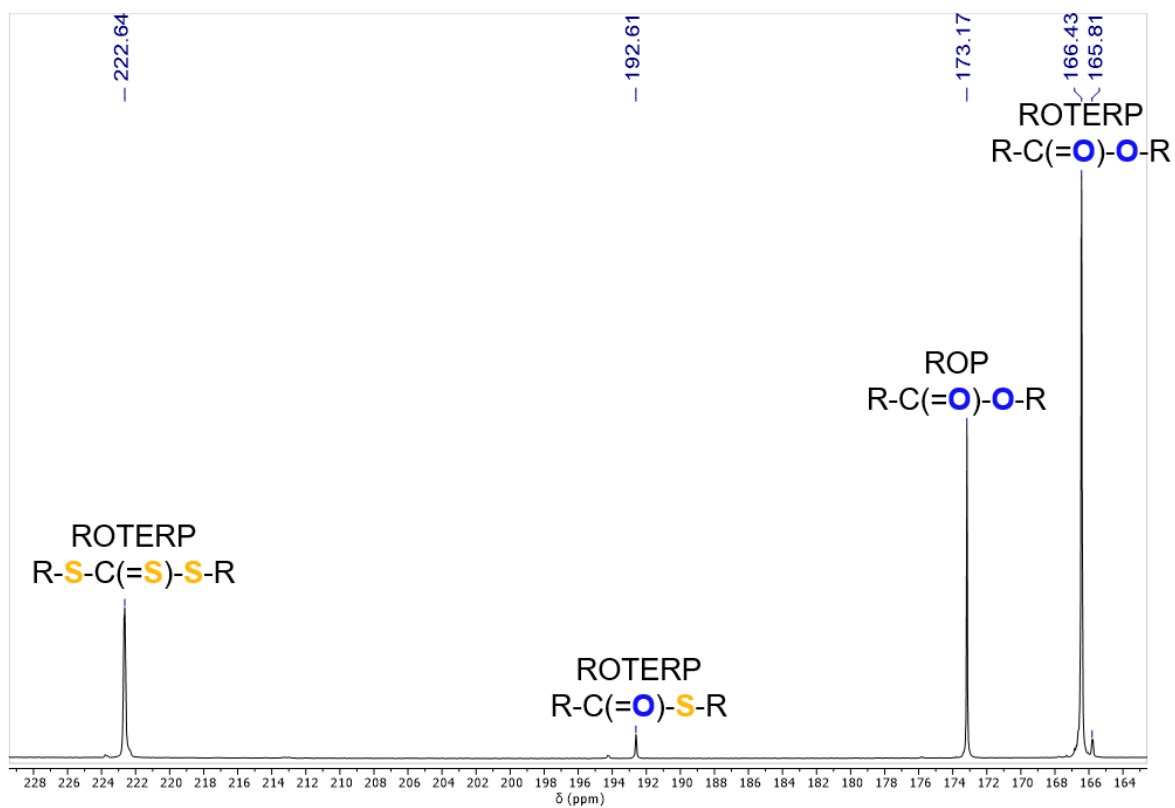


Figure S 55: Zoom into the Carbonyl region of the $^{13}\text{C}\{^1\text{H}\}$ NMR spectrum (126 MHz, CDCl_3 , 25°C) of ϵ DL ROP to PTA/ CS_2 /BO ROTERP polymer.

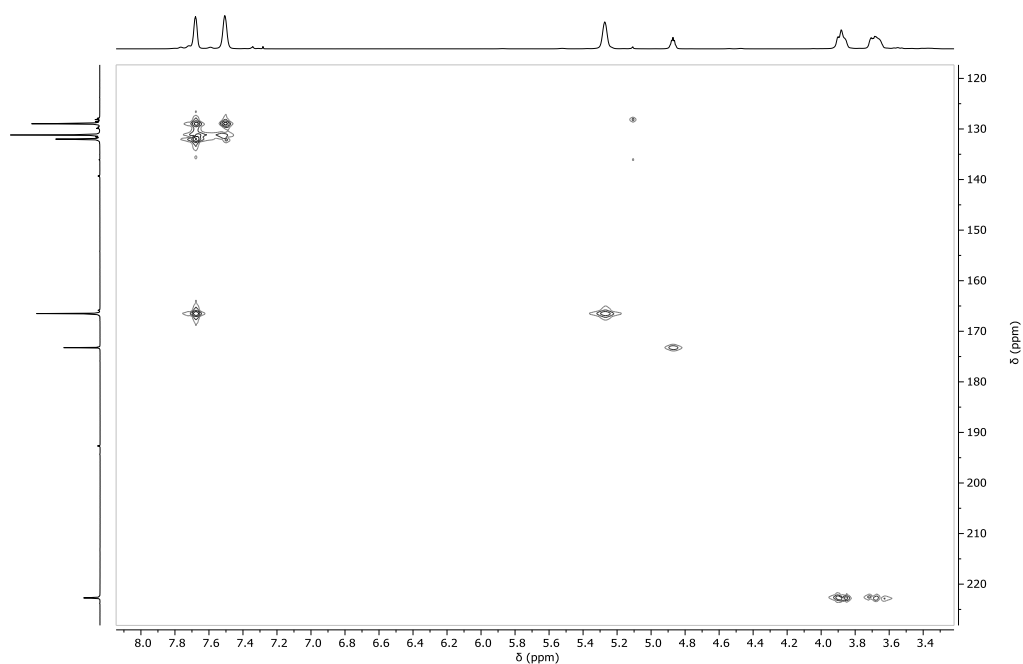


Figure S 56: ^1H - ^{13}C HMBC NMR spectrum (126 MHz, CDCl_3 , 25°C) of ϵDL ROP to PTA/ CS_2 /BO ROTERP polymer.

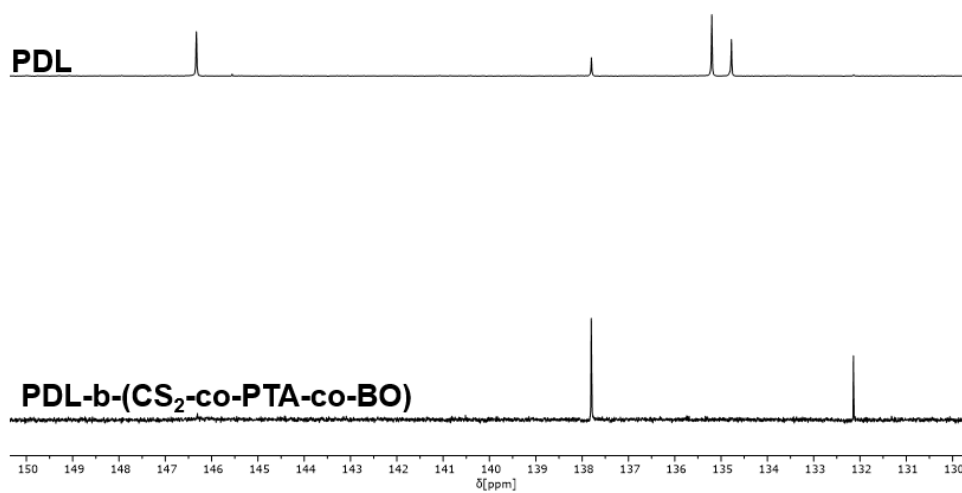


Figure S 57: $^{31}\text{P}\{^1\text{H}\}$ NMR (162 MHz, CDCl_3 , 25°C) end-group analysis before and after mechanistic switch.

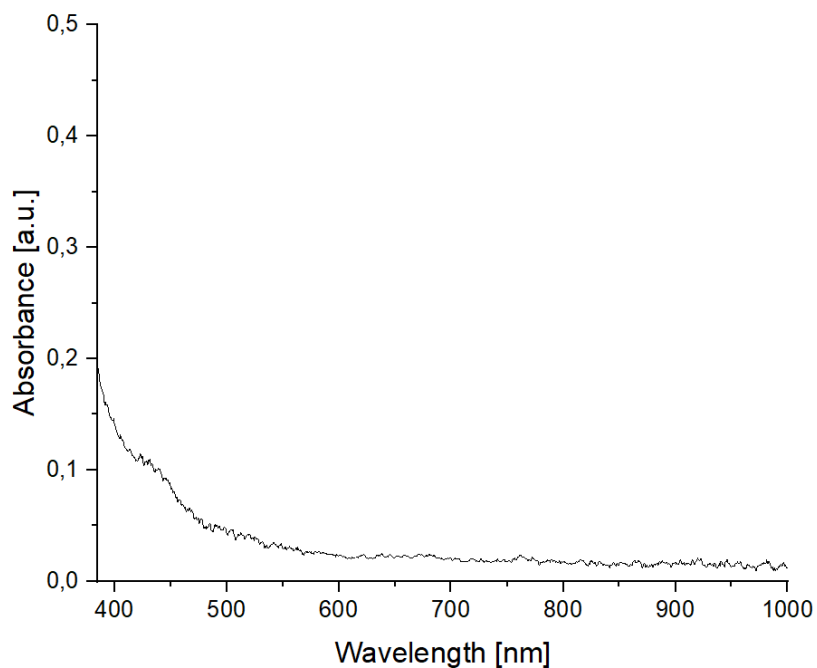


Figure S 58: UV-Vis spectrum of aliquot removed directly after addition of CS₂ and PTA (diluted with appropriate BO/CS₂ mixture by a factor of 10 prior to measurement).

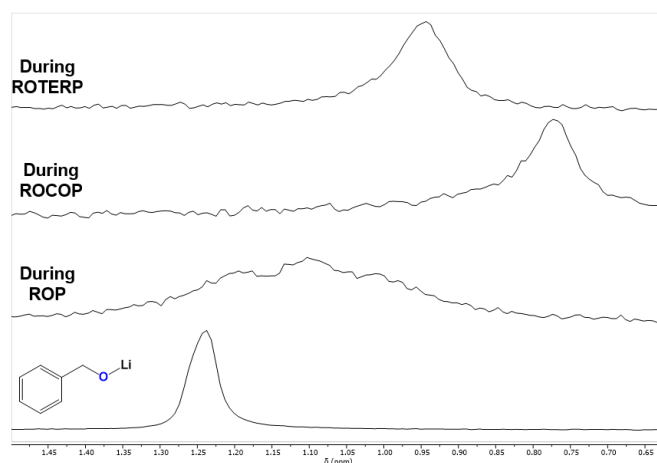


Figure S 59: Overlaid ⁷Li NMR spectra (194 MHz, d₆-Acetone capillary, 25°C) at different stages of switchable catalysis. ROCOP refers to adding CS₂ alone without PTA.

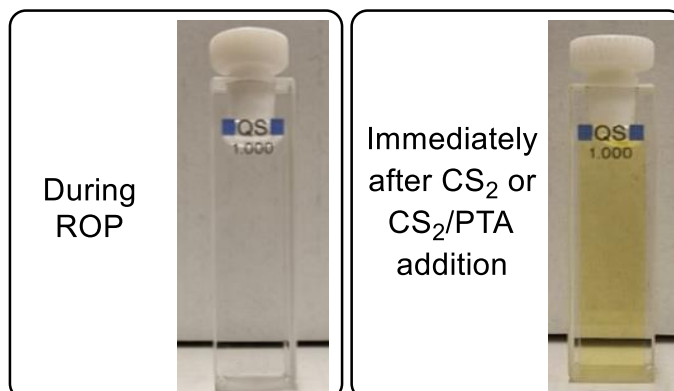


Figure S 60: Reaction colour at different stages of switchable catalysis.

Section S7: Degradation Experiments

UV degradation: The respective polymer (50 mg) was dissolved in CDCl_3 (0.75 mL) and irradiated for 16h by a broadband Hg UV 1000W UV lamp inside a J. Youngs NMR tube. Afterwards the sample was analysed by ^1H NMR spectroscopy and SEC.

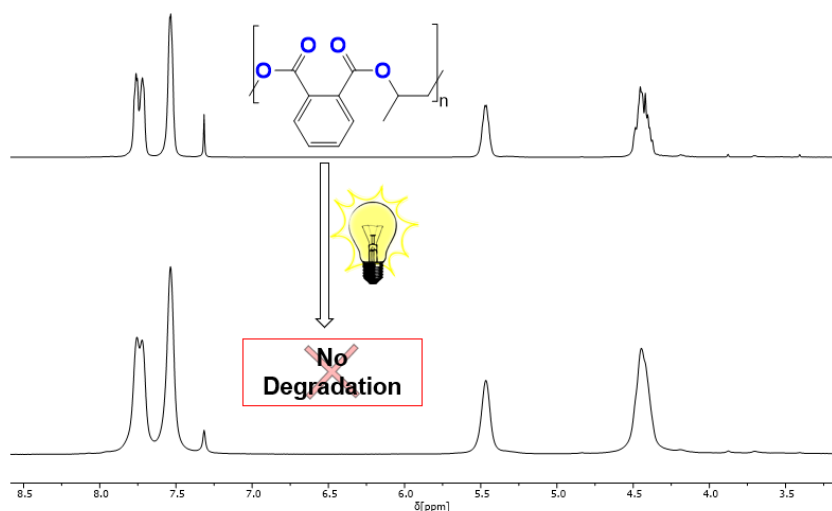


Figure S 61: ^1H NMR spectra (400 MHz, CDCl_3 , 25°C) phtalic anhydride/PO copolymer before and after irradiation with UV-light.

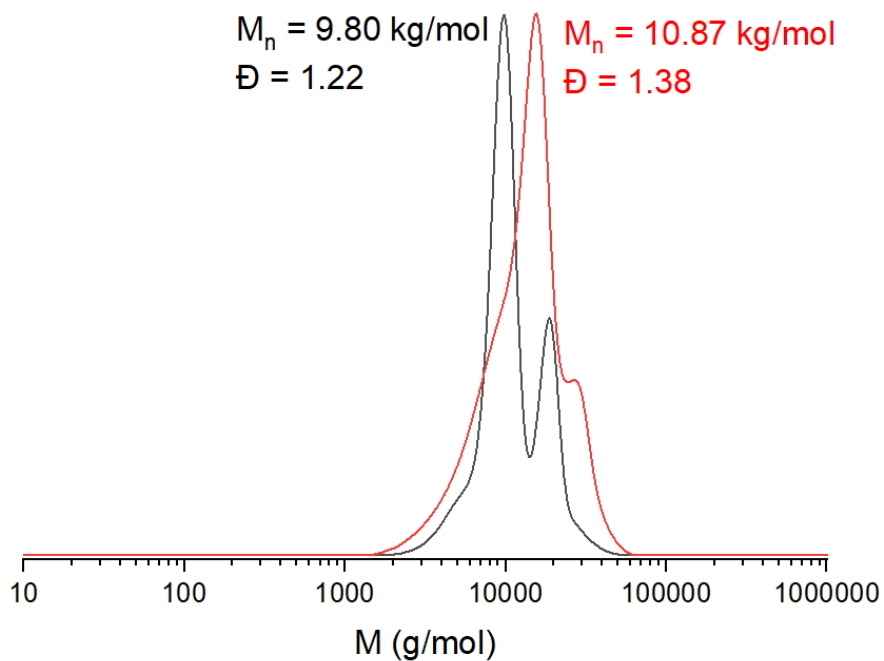


Figure S 62: Overlaid SEC traces of phtalic anhydride/PO copolymer before and after irradiation with UV-light.

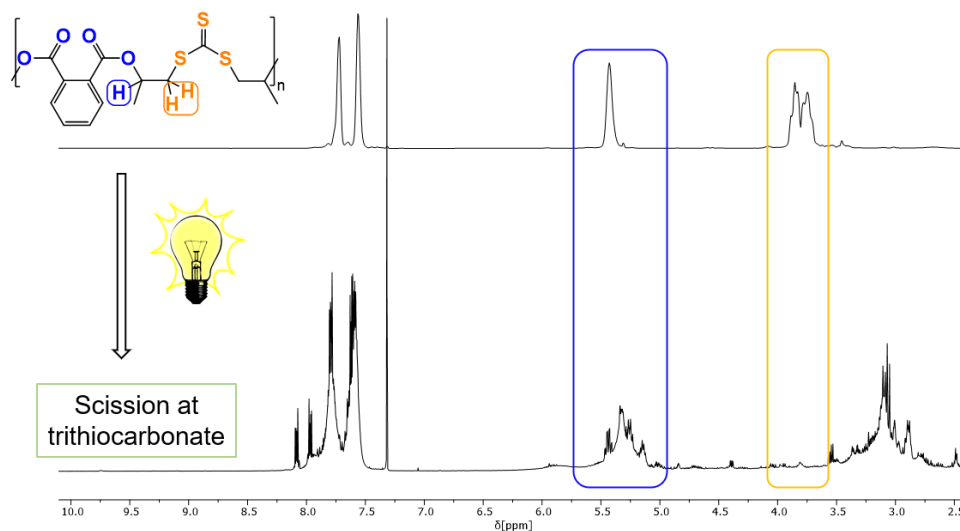


Figure S 63: ^1H NMR spectra (400 MHz, CDCl_3 , 25°C) terpolymer (top) before and (bottom) after irradiation with UV-light.

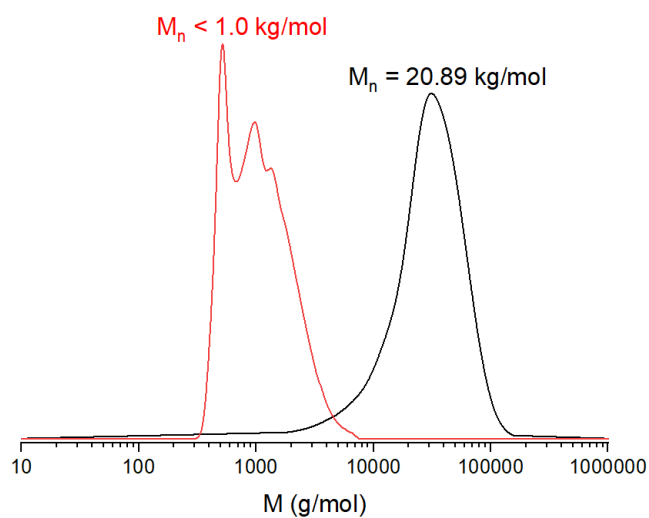


Figure S 64: Overlaid SEC traces before and after UV irradiation of terpolymer before (black) and after (red) irradiation with UV-light

Oxidative degradation: The respective polymer (50mg) was dispersed in aqueous H_2O_2 (3 mL) and stirred for 5d in a glass vial. In case of the polyester, all polymer remained dispersed and SEC as well as NMR remained unchanged. In case of the ROTERP polymer the initial yellow suspension gradually turned into a colourless solution with minor amounts of a colourless precipitate. The suspension was extracted with CDCl_3 , dried over MgSO_4 , filtered and analysed by NMR and SEC.

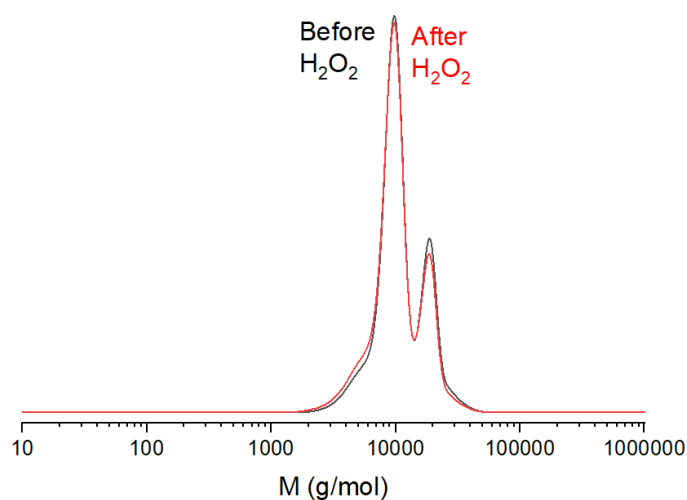


Figure S 65: Overlaid SEC traces of phtalic anhydride/PO copolymer before and after dispersion in H_2O_2 . NMR spectra remains unchanged.

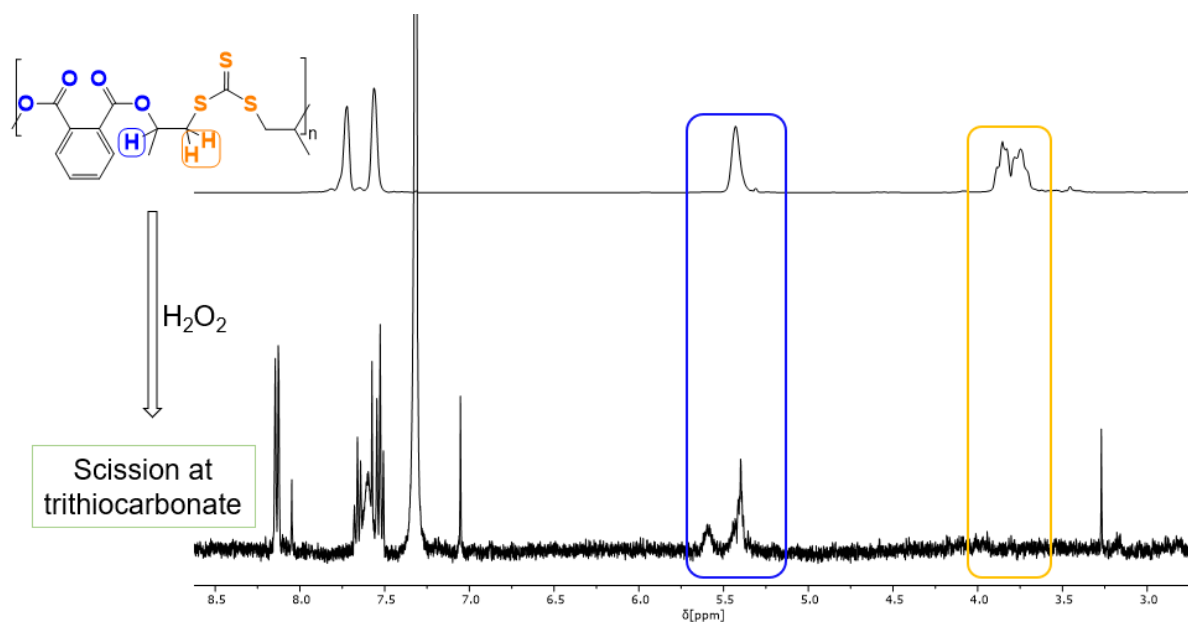


Figure S 66: ¹H NMR spectra (400 MHz, CDCl_3 , 25°C) of terpolymer (top) before and (bottom) after oxidative degradation. No polymeric material could be detected by SEC.

Section S8: Crystallography

X-Ray data were collected on a BRUKER D8 Venture system. Data were collected at 100(2) K using graphite-monochromated Mo K α radiation ($\lambda_{\alpha} = 0.71073 \text{ \AA}$). The strategy for the data collection was evaluated by using the Smart software. The data were collected by the standard " ψ - ω scan techniques" and were scaled and reduced using Saint+software. The structures were solved by using Olex2,^[3] the structure was solved with the XT^[4] structure solution program using Intrinsic Phasing and refined with the XL refinement package^[5,6] using Least Squares minimization. Deposition number CCDC 2151056, contains the supplementary crystallographic data for this paper. These data are provided free of charge by the joint Cambridge Crystallographic Data Centre and Fachinformationszentrum Karlsruhe Access Structures service www.ccdc.cam.ac.uk/structures.

Compound	MTC
Empirical formula	C ₄₀ H ₅₈ Li ₂ O ₁₀ S ₂
Formula weight	776.86
Temperature/K	100
Crystal system	monoclinic
Space group	P2 ₁ /n
a/Å	11.2936(6)
b/Å	21.8827(10)
c/Å	17.1083(7)
α/°	90
β/°	94.544(2)
γ/°	90
Volume/Å³	4214.8(3)
Z	4
ρ_{calc}g/cm³	1.224
μ/mm⁻¹	0.179
F(000)	1664.0
Crystal size/mm³	0.6 × 0.16 × 0.15
Crystal shape	needle
Radiation	MoK α ($\lambda = 0.71073$)

2θ range for data collection/°	4.068 to 50.842
Index ranges	-13 ≤ h ≤ 13, 0 ≤ k ≤ 26, 0 ≤ l ≤ 20
Reflections collected	7771
Independent reflections	7771 [R _{int} = 0.0, R _{sigma} = 0.0235]
Data/restraints/parameters	7771/0/604
Goodness-of-fit on F²	1.116
Final R indexes [I ≥ 2σ (I)]	R ₁ = 0.0472, wR ₂ = 0.0929
Final R indexes [all data]	R ₁ = 0.0561, wR ₂ = 0.0967
Largest diff. peak/hole / e Å⁻³	0.26/-0.24

Compound	MTC^{Na}	MTC^K
Empirical formula	C ₁₂ H ₁₃ NaO ₃ S	C ₉₆ H ₁₀₄ K ₈ O ₂₄ S ₈
Formula weight	260.27	2211.07
Temperature/K	100	100
Crystal system	triclinic	monoclinic
Space group	P-1	P2/n
a/Å	5.9833(6)	15.1783(13)
b/Å	9.3642(10)	6.6961(6)
c/Å	11.7461(12)	30.176(3)
α/°	90.127(4)	90
β/°	101.890(4)	104.412(3)
γ/°	97.726(4)	90
Volume/Å³	637.85(11)	2970.4(5)
Z	2	1
ρ_{calc}/cm³	1.355	1.236
μ/mm⁻¹	0.280	0.492
F(000)	272.0	1152.0
Crystal size/mm³	0.24 × 0.24 × 0.11	0.5 × 0.14 × 0.1
Crystal shape	Colorless	colorless

Crystal color	needle	needle
ion	MoK α ($\lambda = 0.71073$)	MoK α ($\lambda = 0.71073$)
2θ range for data collection/$^\circ$	4.392 to 53.054	4.18 to 50.904
Index ranges	$-7 \leq h \leq 7, -11 \leq k \leq 11, 0 \leq l \leq 14$	$-18 \leq h \leq 18, -8 \leq k \leq 8, -36 \leq l \leq 36$
Reflections collected	2612	48719
Independent reflections	2612 [$R_{\text{int}} = 0.0, R_{\text{sigma}} = 0.0314$]	5700 [$R_{\text{int}} = 0.1002, R_{\text{sigma}} = 0.0441$]
Data/restraints/parameters	2612/0/157	5700/0/314
Goodness-of-fit on F^2	1.054	1.150
Final R indexes [$I \geq 2\sigma(I)$]	$R_1 = 0.0533, wR_2 = 0.1478$	$R_1 = 0.0819, wR_2 = 0.2408$
Final R indexes [all data]	$R_1 = 0.0598, wR_2 = 0.1521$	$R_1 = 0.0829, wR_2 = 0.2420$
Largest diff. peak/hole / e \AA^{-3}	0.48/-0.46	1.85/-0.64

Section S9: Bibliography

- [1] L.-Y. Wang, G.-G. Gu, T.-J. Yue, W.-M. Ren, X.-B. Lu, *Macromolecules* **2019**, *52*, 2439–2445.
- [2] A. Spyros, D. S. Argyropoulos, R. H. Marchessault, *Macromolecules* **1997**, *30*, 327–329.
- [3] O. V. Dolomanov, L. J. Bourhis, R. J. Gildea, J. a. K. Howard, H. Puschmann, *J Appl Cryst* **2009**, *42*, 339–341.
- [4] G. M. Sheldrick, *Acta Cryst.* **2015**, *A71*, 3–8.
- [5] G. M. Sheldrick, *SHELXL Version 2014/7, Program for Chrystal Structure Solution and Refinement*, Göttingen, Germany, **2014**.
- [6] G. M. Sheldrick, *Acta Cryst.* **2008**, *A64*, 112–122.